AN ABSTRACT OF THE THESIS OF

Jennifer L. Fowler for the degree of Master of Science in Veterinary Science presented on June 1, 2017.

Title: Pulmonary Imaging of Dairy Calves with Naturally Acquired Respiratory Disease

Abstract approved:

_____

Susanne M. Stieger-Vanegas

Bovine respiratory disease complex (BRD) is an infection of both the upper and lower respiratory tract and includes components of rhinitis, otitis, tracheitis, and pneumonia. Bovine respiratory disease (BRD) is one of the most common causes of morbidity and mortality of calves in the United States and world-wide. Besides the financial and animal losses, BRD has negative implications for animal welfare. Clinical diagnosis of pulmonary disease in calves with BRD is challenging as clinical respiratory scoring systems, thoracic auscultation, and bronchoalveolar lavage are only moderately sensitive and specific for pulmonary disease detection. Thus, alternative diagnostic testing methods (i.e., thoracic radiography, ultrasonography, and computed tomography) are needed for early detection and treatment of BRD.

Thoracic radiography is the most commonly utilized technique to evaluate the thorax for the presence of pulmonary disease. However, in large animal patients including calves, pulmonary ultrasound is currently more frequently performed due to its ease of use, real time imaging, ability to monitor disease, and availability in field conditions. In human patients, computed tomography (CT) is considered either the gold

standard or method of choice to evaluate for pulmonary disease. This is likely similar in veterinary patients but has not been established yet.

In the first study, the objective was to evaluate if thoracic radiography provides accurate information about the severity and extent of lung disease compared to CT in calves with naturally occurring respiratory disease. The goal of the study was to assess if thoracic radiography could be used as a potential on-farm diagnostic tool for pulmonary disease detection in calves with naturally occurring respiratory disease. As CT is considered the method of choice to for detecting pulmonary disease, it was used as a reference standard. Additionally, we were interested if current clinical respiratory scoring techniques allow for detection of pulmonary disease in acute and chronic pulmonary diseased calves to a similar degree as thoracic computed radiography (CR) and CT.

First, a CT protocol was established utilizing an intravenously injected sedation protocol using xylazine, butorphanol, and ketamine. The feasibility and safety of performing contrast-enhanced thoracic multidetector computed tomography (CT) examinations in sedated calves was evaluated. Finally, radiographic pulmonary disease detection rates were compared with those of thoracic CR and the Wisconsin respiratory scoring system.

Lateral thoracic CR was performed on fifteen awake, standing Jersey calves with acute or chronic respiratory disease as diagnosed on-farm with the Wisconsin respiratory scoring system. Once calves were sedate, thoracic CT was performed pre- and post-intravenous iodinated contrast medium administration using a 64-multidetector CT.

We observed that thoracic CT was superior to CR for pneumonia detection in acute and chronic respiratory diseased calves due to the lack of summation in all areas of the lungs. However, a diagnosis of pneumonia was made with equal rate on both thoracic CR and CT. The intravenous sedation protocol enabled acquisition of CT images of diagnostic quality, without the need for re-scanning. Although mild differences in classification of lung pattern and extent of lung disease were seen when comparing an experienced and a less experienced evaluator, the overall differences were not statistically significant. The best intra- and inter-observer agreement was noted when evaluating the cranioventral aspects of the lungs in either modality. Wisconsin Calf Respiratory Scoring was not able to diagnose chronic pneumonia in calves.

Lung ultrasonography (US) has been used to diagnose and monitor pulmonary disease in large animal veterinary species as well as in humans. In the second study, the objective was to evaluate US as a potential on-farm diagnostic tool for pulmonary disease detection in calves. To accomplish our objective, US lung lesion detection rates of 16 Jersey calves with and 6 Jersey calves without clinical sigs of respiratory disease were compared to those with digital radiography (DR), CT, histopathology, and Wisconsin Calf Respiratory Scoring

In the second study, we observed that lung US was successfully performed in all calves without sedation and in standing position. Clinically healthy calves with low respiratory scores (<2) were diagnosed with pulmonary parenchymal changes on all imaging modalities and histopathologically, but the observed changes were smaller and less severe than in calves with clinical respiratory disease. Accurate assessments of severity and distribution of pneumonia, and differentiation of lung pattern types could be

made with US and correlated well with DR, CT and histopathology. Pulmonary US is an easy to perform, feasible and accurate technique diagnosing pulmonary disease in calves and allows differentiation between clinically healthy and respiratory diseased calves. However, US does not allow identification of intraparenchymal bullae or abscesses.

In this study, thoracic DR, pulmonary US, and thoracic CT performed similarly well for pneumonia detection by each evaluator, and a more experienced evaluator had a better overall sensitivity for pneumonia detection with all imaging modalities. This supports the use of US as a potential diagnostic tool for pneumonia detection in calves.

Pulmonary Imaging of Dairy Calves with Naturally Acquired Respiratory Disease

by
Jennifer L. Fowler

A THESIS

submitted to

Oregon State University

in partial fulfillment of
the requirements for the
degree of

Master of Science

Presented June 1, 2017
Commencement June 2018

Master of Science thesis of Jennifer L. Fowler presented on June 1, 2017

APPROVED:

Major Professor, representing Veterinary Science

Dean of the College of Veterinary Medicine

Dean of the Graduate School

I understand that my thesis will become part of the permanent collection of Oregon State University libraries. My signature below authorizes release of my thesis to any reader upon request.

Jennifer L. Fowler, Author

ACKNOWLEDGEMENTS

I am thankful to: Dr. Susanne Stieger-Vanegas, for the time provided for this masters including serving as the major professor, image analysis, and data interpretation.

Dr. Jorge Vanegas, your time and assistance caring for the calves, and the positivity you exuded during the long drives and days of imaging were crucial to successful completion of the project.

Dr. Rob Bildfell, thank you for agreeing to serve as a member of my graduate committee. Your efforts in study design and completion of the gross and microscopic examinations was vital for ensuring a quality study.

Dr. Gerd Bobe, thank you for serving as my Graduate Council Representative and ensuring the degree requirements were met. Without your enthusiastic statistical assessments, this project would be a mere table of coded notes.

In addition to my graduate committee, I am indebted to Jason Wiest and Cynthia Viramontes for their help calf handling and acquiring images. You came in early, left late, and provided laughter through every tough day.

To my many House Officer comrades, especially Mark Iodence, Emma Gordon, Stephanie Grissom, Rose Baker, Kirsty Husby, and Lauren Newsom, your support and commiseration through plane “crashes,” medical disasters, and many difficult times will never be forgotten. You have become like family and I can never thank you enough.

CONTRIBUTION OF AUTHORS

Comparison of Thoracic Radiography and Computed Tomography in Calves with Naturally Occurring Respiratory Disease

Drs. SM. Stieger-Vanegas and J. Fowler made substantial contributions to the design of the study, data acquisition, analysis and interpretation. Drs. JA. Vanegas and KP. Poulsen made substantial contributions to the design of the study, data acquisition and interpretation. G. Bobe made substantial contributions to the design of the study, analysis and interpretation.

Comparison of Thoracic Radiography, Computed Tomography, and Ultrasound to Histopathology for the Diagnosis of Respiratory Disease in Dairy Calves

Drs. SM. Stieger-Vanegas and J. Fowler made substantial contributions to the design of the study, data acquisition, analysis and interpretation. Drs. JA. Vanegas and R. Bildfell made substantial contributions to the design of the study, data acquisition and interpretation. G. Bobe made substantial contributions to the design of the study, analysis and interpretation.

Financial support was provided by the Department of Clinical Sciences of the College of Veterinary Medicine at Oregon State University and the Veterinary Ultrasound Society of the American College of Veterinary Radiology.

TABLE OF CONTENTS

TABLE OF CONTENTS (Continued)

Page

TABLE OF CONTENTS (Continued)

Page

TABLE OF CONTENTS (Continued)

Page

LIST OF FIGURES

Figure Page

LIST OF TABLES

LIST OF TABLES (Continued)

This work is dedicated:

In loving memory of my parents, Fred and Doreen Fowler.
My parents provided unending support for every endeavor I embarked upon. Through their last moments, they insisted I push forward to focus on completing this thesis and my residency, for the advancement of self and science. Without their love and guidance, I could not have made it this far, and without them I don't know what the future holds. They planted the seed for my love of cattle and did all they could to encourage my passion for medicine even when they didn't understand it. I am forever thankful to have had them instilling in me the strength to endure this process, believing in me even when I failed, and teaching me to embrace the fear of long distances and new challenges.

To Morgan and Parker, for being my companions, reminding me to find joy even in dark times, and constantly loving me despite my shortcomings.
You make me a better person.

Chapter 1- Introduction

1.1Respiratory Disease in Calves

1.1.1 Overview

Bovine respiratory disease complex (BRD) is an infection of both the upper and lower respiratory tract and includes components of rhinitis, otitis, tracheitis, and pneumonia.(1) It is commonly encountered in both dairy, feedlot, and backgrounding facilities.(2,3) In addition to being commonly encountered throughout the United States, it is recognized as a worldwide problem.(4–6)

Pathogens associated with BRD vary by facility and region, but often involve bacterial and viral co-infections including but not limited to: *Mycoplasma bovis, Pasteurella multocida, Histophilus somni, Mannheimia haemolytica*, bovine respiratory syncytial virus, bovine viral diarrhea virus, and bovine parainfluenza-3.(7,8) *Pasteurella multocida* has been implicated as the most common pathogen in bovine respiratory disease.(9) A synergistic effect has been shown between *Mycoplasma bovis* and *Pasteurella multocida*.(10) Respiratory disease is often precipitated by a viral infection, which alters the immune system, inciting immune compromise and leading to secondary bacterial pneumonia.(11) Time periods of high stress, such as shipping or surgical procedures particularly in the peri-weaning period, have been recognized as cofactors for immune suppression which may trigger the onset of disease and worsen the overall response to treatment.(12)

1.1.2 Importance of Bovine Respiratory Disease in the United States Food Production Industry

In addition to the animal welfare concerns associated with bovine respiratory disease, the condition is the most prevalent cause of morbidity and mortality in feedlot cattle with up to approximately 13% of the animals being diagnosed with respiratory disease.(3) In calves, respiratory disease is the second most common cause of morbidity prior to weaning and the most common cause of morbidity post-weaning, affecting approximately 12% and 6% respectively, and in some facilities up to 100% of the dairy calves having been treated with antibiotics prior to weaning.(13) Although precise financial losses are difficult to account for, it is estimated that in the United States each case of respiratory disease in feedlots costs approximately $20-77,(9) with the overall cattle industry losing at least $500-900 million per year due to respiratory disease complex.(14,15)

Early diagnosis of disease is essential to reduce the negative impacts of the disease in the population, to improve the treatment response and to decrease the financial losses due to treatment failure and animal losses due to death and culling from the herd. Furthermore, early diagnosis promotes good quality of life for the patient and improves response to treatment.(8,16–18) Juvenile pneumonia in cattle has been shown to have the potential for lifelong impacts potentially resulting in decreased milk and carcass production.(9,19)

1.2 Bovine Respiratory Anatomy and Physiology

In cattle, the lungs are comprised of six major lobes: the right cranial, right middle, right caudal, accessory, left cranial and left caudal lung lobes. Both the right

cranial and left cranial lung lobes have distinct intralobar fissures causing these lobes to have cranial and caudal parts, which is not seen to the same degree in dogs or horses. The right lung, comprised of the four lobes described, is larger than the left lung.(20)

The lung is peripherally covered by a thin mesothelial layer called the visceral pleura. The bovine pleura is thick, similar to that of the human lung, and has extensions into the central parenchyma which causes well-defined sub-lobules that can be seen on gross examination (Fig 1-1).(21) The micro-anatomic structure of the bovine lung is similar to the human lung, in that the thick visceral pleura of the lung is contiguous with the interlobular septal interstitium, which divides the lobes into primary and secondary lobules.(26, 27) In species with thick pulmonary visceral pleura, including cattle, horses, and humans, the bronchial artery serves as the primary blood supply to the pleura. In species with thin pulmonary visceral pleura, such as the dog and cat, the pulmonary arteries are the primary blood supply to the pleura. Additionally, thin layers of fibrous connective tissue are present between the alveoli and respiratory bronchi of cattle and humans which prevents cross absorption of gas between adjacent lobules, which is in contrast to the small animal patient in which a lack of fibrous tissue between the acini allows for oxygen absorption between non-contiguous respiratory airways and alveoli.(24) In the human lung, pulmonary lobules are comprised of 3-30 acini, the functional unit formed by numerous alveoli, but this has not been elucidated in bovids.(25)

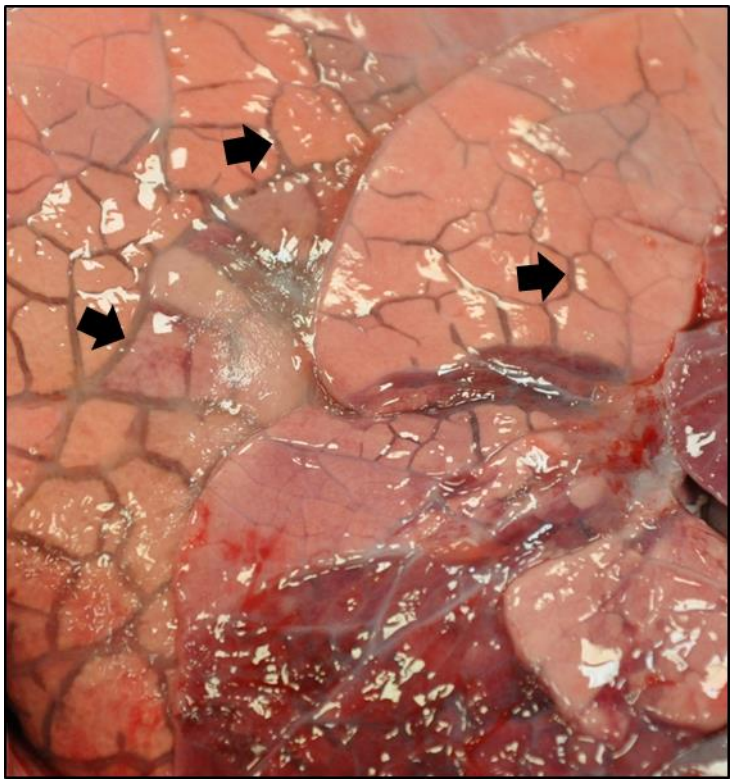

Figure 1-1: Interlobar septal edema. An increased distinction of the intralobular fissures due to edema in a calf with severe, chronic respiratory disease. The widened, edematous intralobular fissures (black arrows) causes the cobble stone pattern of the lung parenchyma to be prominent in diseased aspects of the lung.

In contrast to the branching of the trachea seen in small animals, ruminants have a cranial branch from the right ventrolateral aspect of the trachea approximately 10 cm cranial to the bifurcation, known as the tracheal bronchus (Fig 1-2).(26) This tracheal bronchus serves the cranial and caudal parts of the right cranial lung lobe, and bifurcates near the hilum of the right cranial lung lobe.(20) The ventrolateral position of the tracheal bronchus causes the right cranial lung lobe to be more susceptible to pneumonia, especially secondary to aspiration. This is in contrast to the pattern of pneumonia seen in dogs and cats, in which the right middle lung lobe is at increased risk due to the more

cranioventral position of the segmental bronchus to the right middle lung lobe which branches from the right caudal principal bronchus.(27)

Figure 1-2: Three-dimensional (3D) CT reconstruction of the trachea, bronchi and incompletely air-filled lung of a juvenile dairy calf with severe respiratory disease viewed from ventral. The right and left cranial lung lobes are not 3D reconstructed, due to a lack of air filling, which leads it to be removed from the reconstruction thereby allowing the tracheal bronchus to be seen supplying the right cranial lung lobe (white arrow). The tracheobronchial bronchus originates from the ventrolateral trachea approximately 10 cm cranial to the tracheal bifurcation (white chevron).

In addition to the anatomical variation seen in the bronchial tree of the bovid, a general physiologic predisposition to the development of pneumonia has been suggested. Cattle are known to have a larger basal airflow volume, despite a similar tracheal volume to total lung volume proportion when compared to the horse.(22) This larger airflow volume is thought to provide an increased pulmonary exposure to pathogens when compared to other mammalian species.

1.3 Clinical Assessment

1.3.1 Physical Examination

Calves with respiratory disease often present with fever, cough, and tachypnea. Because of this, the physical examination comprises the primary method of evaluating calves presumed to have respiratory disease. Three physical examination characteristics are used as principal identifiers for calves with respiratory disease: depression of attitude, inappetence causing a loss of ruminal fill, and altered respiratory rate and effort/quality.(28) Calves identified as ill based on these findings are often removed from their cohort for treatment and further monitoring.

Implementation of surveillance protocols for animal monitoring is employed in many herd systems. In very large herds, hands on examination with thoracic auscultation of each at risk individual can be overly time-consuming for farm veterinarians and animal caretakers. Testing such as diagnostic imaging, microbiology, and clinical pathology may be costly and time consuming for assessing individual animals, and even more-so when being utilized in a large cohort for disease monitoring. To mitigate this, assessment methods heavily relying on visual inspection have been designed to allow for

identification of calves likely infected with BRD and in need of further evaluation and/or treatment. The first respiratory scoring system was described in 1977 by Thomas et al.(29) In this system, 17 categories of clinical and hematologic status were assessed including: apathy, anorexia, nasal discharge, adenitis, ocular discharge, conjunctivitis, dyspnea, wasting, cough, diarrhea, respiratory rate, temperature, erythrocyte count, leukocyte count, mean corpuscle volume, packed cell volume, and hemoglobin. For the clinical categories, scores were assessed either of a 0-1 or 0-3 scale; body temperature and hematologic scores were summed, and each category then had a weighting system applied before summing for a final score. As such, the system was bulky and required blood testing, and has since been replaced by simpler scoring systems.

The most common currently utilized clinical assessment method for identifying and prognosticating respiratory disease in calves is the Wisconsin Calf Score.(30) For this method, a score of 0-3 is assigned based on severity (0=normal, 3=most severe) for body temperature, cough, nasal or ocular discharge, and ear position or head tilt. The maximum possible score is 12. This method is much simpler to utilize and therefore allows to easily train farm workers on site. Furthermore, no additional laboratory testing is required, which is financially beneficial. However, depending on the examiner, respiratory scoring has been shown to have a suboptimal sensitivity and secondarily a high false-negative rate.(31) Therefore, accurate diagnosis of bovine respiratory disease remains a challenge.

1.4 Pathology and Microbiology

Postmortem examinations are often performed in large production facilities as a means of disease monitoring and etiologic diagnosis. The procedure is so common that

professionally developed websites are available to guide producers with instructions in performing the task in the absence of a veterinarian if needed.(32,33)Thorough gross carcass examination allows for a global overview of the body systems, but histopathology is typically needed for disease classification. When delays in tissue sampling are encountered between the time of death and completion of a necropsy, tissue samples may deteriorate, decreasing the diagnostic capabilities of the tests. When completed in a timely manner, with proper samplehandling, histopathology of lung has been shown to aid in identification of unexpected micro-organisms in combination with histologic patterns of change.(34) Limitations to the successful use of necropsy for disease monitoring include potential incomplete or misleading clinical history, inadequate sample preservation, and incomplete carcass examination.(35) As well, the potential risk of exposure of the evaluator to zoonotic agents or of personnel injury must also be considered when assessing the usefulness and limitation of necropsy as a diagnostic test.(36)

Airway sampling is sometimes attempted as an antemortem diagnostic test to elucidate the cause of pulmonary changes detected by diagnostic imaging. Trans-tracheal wash will allow for collection of fluid that originates from both lungs, whereas bronchoalveolar lavage (BAL) provides a sample from a focal portion of a specific lung lobe.(37) More variation is seen in the cell populations obtained by trans-tracheal wash, but the focal origin of the fluid acquired by BAL may lead to under-representation of disease. (38) Additionally, in severely compromised patients, anesthesia might be necessary for a BAL, which may pose further risks of mortality in severely compromised patients, incurs higher costs for the procedure and testing of BAL fluid, these may be

limiting factors in acquiring BAL samples in production animals, particularly in large herd settings.

1.5 Respiratory Imaging

1.5.1 Radiography

Thoracic radiography is the most commonly used test to evaluate for pneumonia in human and veterinary patients. Due to the size of the patient, and the x-ray output limitations of equipment available for radiography in the field, thoracic radiography of cattle is typically often limited to juvenile patients. When thoracic radiography is attempted in calves, standing lateral projections are typically obtained without an orthogonal view, due to equipment output and animal handling limitations.(39) Despite the limitations of image acquisition, the practicality of utilizing thoracic radiography in field conditions due to the low cost and widespread availability make it a commonly used technique for assessment of respiratory disease in large animals.(40,41)

Due to summation of structures, radiography can be inaccurate in assessing distribution and severity of disease. In humans bedside thoracic radiography has been shown to be inadequate in some patient for identification of pulmonary disease.(42) In a human study of 47 patients with community-acquired pneumonia, eight pneumonia cases were diagnosed as negative with thoracic radiography alone, and ten cases of bilateral pneumonia were inaccurately diagnosed as having unilateral pneumonia only utilizing thoracic radiography.(43) No similarly designed studies are available to assess the accuracy of thoracic radiography in calves with pneumonia.

Several descriptive studies describing the radiographic findings associated with bovine pneumonia identified on thoracic film radiography are available for

reference.(41,44,45) These studies apply the method of pulmonary pattern recognition [bronchial, interstitial (unstructured vs. structured), alveolar, and vascular] as the mainstay of assessment. The overlap between the radiographic pulmonary changes suggestive of pulmonary infection and both benign changes such as atelectasis from prolonged recumbency or diseases of non-pulmonary origin such as cardiogenic pulmonary edema remains a concern in cases in which a thorough physical examination cannot be completed.

Although radiation exposure may be considered of less importance in a patient intended for slaughter, the exposure of human handlers must still be considered when planning diagnostic procedures in food animals. Particularly, when large numbers of patients require assessment and manual restraint is necessary, secondary radiation exposure to human handlers could be substantial. Several studies have been performed to assess the exposure of personnel during equine radiography, but no similar studies have been completed in cattle.(46,47) Regardless, given that health implications of radiation exposure are considered stochastic, with no minimal safety threshold, exposure is closely monitored in the working environment and efforts to reduce the overall exposure are employed to conform to the ALARA (as low as reasonably achievable) principle. Due to the risks associated with radiation exposure, continuous development of equipment requiring lower radiation exposure to create an image of similar diagnostic quality and diagnostic techniques for assessment of herds at risk of developing or exhibiting clinical signs of bovine respiratory disease which do not utilize ionizing radiation are preferable.

1.5.2 Computed Tomography

It is recognized in human literature that a true "gold standard" for diagnosis of pneumonia does not exist.(48) Computed tomography(CT) of the thorax is considered the modality of choice to evaluate for the presence of lung disease in human patients.(49) Thoracic CT in dogs has proven to be helpful for evaluating the extent of pulmonary disease and was shown to provide better anatomic detail of the lungs due to a lack of superimposition of anatomical structures.(50) In humans, it was demonstrated that thoracic radiography was inadequate for diagnosing pneumonia and is therefore often replaced by thoracic CT. In human patients, high resolution CT (HRCT) has been shown to enable differentiation between lobar and bronchial pneumonia, as well as between bacterial and atypical pneumonias.(43) High resolution CT images are dissimilar to conventional CT images in that they are made by obtaining thin slices of 1-2 mm thickness, and applying a high-frequency (edge sharpening) algorithm to improve spatial resolution, thereby allowing delineation of structures as small as 0.5 mm in size as distinct, whereby traditional CT images are created from slices up to 10 mm in thickness.(51) Although commonly used in humans,(52) and being described in dogs,(53) HRCT has not been described in ruminants.

The size and conformation of the adult bovine and equine patient impedes the use of CT for assessment of the thorax and abdomen in many large animal patients. However, in juveniles and small/dwarf breeds such as the American Dexter and Miniature Horses, the equipment limitations may not be an issue. Several reports describe the use of CT for thoracic examination in foals(54) and calves,(55) as well as for the diagnosis of discospondylitis in a calf,(56) conformational assessment of the calf pelvis,(57) and

examination of the tympanic bulla of calves(58) have been published. However, the use of computed tomography in calves is often limited by the cost and lack of availability of a CT scanner close to a calf rearing operation.

Furthermore, in veterinary species, CT examinations of the thorax are usually performed using anesthesia with endotracheal intubation to allow using breath-hold techniques, which decrease the risk of respiratory motion in the images.(59) In humans, a physical status scale has been utilized to assess anesthetic risk prior to surgical procedures requiring anesthesia.(60) Utilizing this scale, patients with significant compromise due to overt disease, particularly respiratory disease and fever, are considered at higher anesthetic risk with a physical status scale of 4.(61) If a similar degree of anesthetic risk is assumed in calves with respiratory disease, then utilizing general anesthesia to enable thoracic CT may also be undesirable. Awake and sedation CT scanning protocols have been described for cats with upper airway obstruction(62) and intrathoracic disease,(63) as well as dogs with laryngeal paralysis,(64) acute abdominal signs,(65) and dogs with pelvic fractures from trauma.(66)To date, the only report describing the CT findings of respiratory disease in calves with pneumonia was performed on patients with experimentally induced disease and utilizing a general anesthesia protocol with the patients intubated.(67) A second study was performed to describe the pulmonary parenchyma of normal calves from birth to 105 days of age; however, during the course of this study, four of the six calves developed signs of respiratory disease, and general anesthesia was utilized for CT image acquisition.(55) Neither awake nor sedated CT protocols have been evaluated in calves to date.

When CT of the thorax is available, there are multiple pulmonary assessment paradigms available to consider utilizing. Two potential methods include utilizing the pattern descriptors used in radiographic evaluation to CT images or applying the descriptors proposed in the Glossary of Terms for Thoracic Imaging(68) by the Fleischner Society, an international and multidisciplinary group focused on thoracic diagnostic imaging. In a study of normal foals comparing thoracic radiography and CT, radiographic pattern descriptors [bronchial, interstitial (unstructured vs. structured), alveolar, and vascular] were utilized in the descriptive image analysis.(69) This study found that interpretation of thoracic CT in healthy foals may be less subjective than thoracic radiographic evaluation, with lung attenuation and CT image scores being positively correlated (r= 0.872). Several small animal studies have attempted to apply Fleischner Society descriptors of pulmonary parenchymal changes with mixed results. In one study of canine eosinophilic bronchopneumopathy and a study of canine interstitial pulmonary fibrosis, the "crazy paving" cobblestone-like pattern of increased attenuation of the parenchyma overlying a thin reticular pattern classically identified in human patients was found to be absent in dogs.(70,71) The reason for dogs lacking this pattern on CT was not extrapolated on, but likely originates in the histopathologic differences between the lung of small animals and humans, in which the pleura does not extend centrally into the lung parenchyma of dogs and cats. Given that the microanatomy of the bovine lung is more similar to the human lung, the utilization of a pulmonary pattern paradigm including "crazy paving" and other descriptors defined in the Fleischner Society glossary may be more appropriate than in dogs and cats.

It is noteworthy, that of the CT imaging based pulmonary literature available in veterinary patients, the patient numbers are generally low with some studies including as few as 6 animals.(55,72) Some studies lack definitive diagnosis via histopathology in some or all of the included patients,(71) and diagnostic accuracy is rarely assessed with most focusing on descriptive assessments of disease.(73) It has been stated that in dogs and cats specific patterns of lung change due to pulmonary infectious and inflammatory processes are incompletely established.(74) This is likely to be more of an issue in cattle, in which scant CT data are currently available. Given that CT is considered a reference standard in human medical diagnostics for pulmonary disease, further assessment of calf respiratory disease by CT examination is warranted, if only to assess potential use as a research testing standard.

1.5.3 Ultrasonography

Lung ultrasound has gained more interest and use in the last 5-10 years. Lung ultrasound is frequently used as a first technique in patients with respiratory distress to differentiate between respiratory and non-respiratory causes, to discriminate between lower and upper causes for respiratory disease, and to evaluate a potential for cardiac involvement. For human, especially pediatric patients, ultrasound (US) is preferred for monitoring of disease due to avoidance of exposure to ionizing radiation and the reported high sensitivity of the modality.(42) In the assessment of large herds of cattle, the avoidance of ionizing radiation to staff, farm workers, and veterinarians is likely a substantial benefit to other imaging modalities. As well, given the previously described limitations of portable x-ray generator output, in adult cattle US allows for examination of the thorax which may otherwise be impossible. In humans and adult large animals,

thoracic ultrasonography has been utilized for diagnosis of pulmonary disease and monitoring of treatment response for at least two decades. US examination of the lungs also allows for dynamic examination over the entire phase of the respiratory cycle, whereas radiography allows for examination at a single moment in time, preferably at full inspiration. In a study of children with community acquired pneumonia, ultrasound was found to be more sensitive for detection of disease when compared to radiography.(75)

In pulmonary US, a normal lung interface is seen as an A-line, which is an evenly spaced linear, hyperechoic line seen in parallel to the pleural surface of the lung.(76) The most commonly described abnormal finding is the B-line (also referred to as a "comet-tail"),(77) which is a hyperechoic striation seen coursing perpendicular to the pleural surface. In regions of more severely diseased lung, B-lines may become confluent and develop a region of "white lung".(78) Hepatization or consolidation ('tissue" sign),which represents lung that has a severe loss of air-filling to the point of causing the lung to look similar to the parenchyma of the liver.(77) In regions that only a portion of a lung lobe is consolidated, a "shred sign" is described in which the consolidated region of lung is surrounded by an irregularly shaped region or normally air-filled lung with a resulting strong reverberation artifact.(79) There is some variation in the use of US artifact terminology for describing pulmonary parenchymal changes with a secondary inconsistency in literature descriptions. An example of this variation is the use of the terms "comet-tail", ring-down, and B-lines to represent the perpendicular hyperechoic striation seen extending abnormally from the pleural margin in abnormal lung ultrasounds. Given the inconsistencies in the veterinary literature and overlap seen in medical physics textbooks, the term B-line will be used throughout this work to describe

perpendicular reverberation artifacts both with numerous evenly spaced parallel striations that taper distally causing a mildly triangular shape,(80) and a homogeneously hyperechoic striation lacking in distal tapering.(77)

The most commonly reported short-coming of US examinations is the user (operator/observer) dependent nature of the modality.(81–84) Currently no studies are available directly assessing the impact of user training on the accuracy or diagnostic quality of thoracic US of veterinary patients, specifically in the calf. Specific ultrasound training for evaluators may be important as acquisition of US images of the pulmonary parenchyma of good diagnostic quality requires both comprehension of US physics and frequent modification of machine settings such as imaging depth and focal point. Subtle changes to imaging parameters such as the time-gain compensate setting may play a large role in lesion conspicuity and artifact mitigation, hence the ability to assess the image actively during examination of the patient while adjusting these settings is highly important.(85) Secondly, due to the dynamics of the respiratory cycle, constant assessment of the lung is occurring in tandem with image acquisition. Although several reports of thoracic US of calves are available, the impact of user experience on image acquisition and assessment is not yet known.

A second concern with respect to implementing thoracic US as a primary tool in the pulmonary examination paradigm is regarding the depth of assessment possible. Almost every report discussing the use of US for pulmonary examination suggests that the presence of aerated lung precludes the assessment of the parenchyma by creating a reverberation artifact. This artifact occurs due to the difference in the attenuation of sound by the lung when compared to soft tissue,(80) the standard to which diagnostic US

machines are set to interpret data and develop an image. When regions of consolidation or nodules are present deep to normally air-filled lung, the presence of this normal reverberation artifact may impede identification of the deeper structures. However, recent publications suggest that US may be useful for assessing the lung parenchyma in cases of bronchiolitis,(86) and pulmonary fibrosis,(87) and has been shown to be a useful tool for differentiating acute pulmonary edema in pregnancy from an exacerbation of asthma in humans.(88) Recently in the veterinary literature, three reports of utilizing thoracic US for the evaluation of the pulmonary parenchyma for the presence of pulmonary edema due to congestive heart failure, have been published.(89–91)

Of the bovine lung US studies currently available, confirmatory testing for the presence of pulmonary disease lacks uniformity. Some studies have compared US to bronchoalveolar fluid analysis(92), clinical scoring(8), and thoracic auscultation(93) in the absence of a high-performing reference standard despite recognizing these tests have a moderate performance at best. As well, in the current body of literature, when histopathology was utilized, random samples were obtained without attempts to correspond the US findings with the location of the tissue sample collections, or sometimes without histopathology having been performed.(94,95) Due to this, comparison or confirmation of the histopathology results with the US abnormalities was not possible.

To date, no study has been performed comparing thoracic radiography, computed tomography, and ultrasonography to the reference standard of histopathology in a single cohort of calves with and without clinical respiratory disease.

1.5.4 Comparison of imaging modalities for evaluating the lungs in bovine patients

Each diagnostic imaging modality described has benefits and limitations (Table 1-1). In bovine lung imaging, the modality selected for use is often dependent on the availability at the facility the animal is located at or the operator preference in locations in which multiple options are available. Radiography and thoracic ultrasound tend to be the first techniques employed for evaluating the lungs in bovine patients due to wide availability and ease of use. Computed tomography is often limited to larger hospitals and research facilities, and as such is not considered a first line imaging technique for bovine patients with respiratory disease.

	Benefits	Limitations
Radiography	-Widely available - Relatively inexpensive - Easy to use	- Equipment output limitations for large, adult animals - May not be able obtain orthogonal projection, especially in adult animals - Summation of structures - Radiation exposure for personnel
Computed Tomography	-Eliminates structural summation - Allows for 3D reconstruction and parenchymal/functional assessment with contrast administration. - Currently in human patients and likely also in veterinary patients considered gold standard for evaluation of the lungs.	-Very limited availability - Costly for study acquisition and interpretation - High ionizing radiation exposure for patient +/- personnel - Often requires at least sedation or general anesthesia - No CT scanner available allowing for examination of a regular adult sized bovine, therefore experiences are limited to young or small sized bovines.
Ultrasonography	-Readily available - Very sensitive to tissue interfaces and presence of fluid or gas - No patient or personnel exposure to ionizing radiation - Can be performed in awake standing patient	- Can be time consuming for image acquisition. - Operator dependence for quality of imaging study

Table 1-1: Comparison of the benefits and limitations of the various imaging techniques evaluating the lungs in bovine patients.

1.6 References

1. Love WJ, Lehenbauer TW, Van Eenennaam AL, Drake CM, Kass PH, Farver TB, et al. Sensitivity and specificity of on-farm scoring systems and nasal culture to detect bovine respiratory disease complex in preweaned dairy calves. J Vet Diagn Invest [Internet]. 2016;28(2):119–28. Available from: http://vdi.sagepub.com/content/28/2/119
2. Cernicchiaro N, White BJ, Renter DG, Babcock AH. Evaluation of economic and performance outcomes associated with the number of treatments after an initial diagnosis of bovine respiratory disease in commercial feeder cattle. Am J Vet Res. 2013;74(2):300–9.
3. USDA Veterinary Services - Centers for Epidemiology and Animal Health.

Feedlot 2011: Types and Costs of Respiratory Disease Treatments in U.S. Feedlots [Internet]. 2013. Available from: https://www.aphis.usda.gov/animal_health/nahms/feedlot/downloads/feedlot2011/Feed11_is_RespDis.pdf

4. Thompson PN, Stone A, Schultheiss WA. Use of treatment records and lung lesion scoring to estimate the effect of respiratory disease on growth during early and late finishing periods in South African feedlot cattle1. J Anim Sci [Internet]. Madison, WI: American Society of Animal Science; 2006;84:488–98. Available from: http://dx.doi.org/10.2527/2006.842488x
5. Jones C, Chowdhury S. Bovine herpesvirus type 1 (BHV-1) is an important cofactor in the bovine respiratory disease complex. Veterinary Clinics of North America - Food Animal Practice. 2010.
6. Hay KE, Morton JM, Mahony TJ, Clements ACA, Barnes TS. Associations between animal characteristic and environmental risk factors and bovine respiratory disease in Australian feedlot cattle. Prev Vet Med. 2016;
7. Grissett GP, White BJ, Larson RL. Structured Literature Review of Responses of Cattle to Viral and Bacterial Pathogens Causing Bovine Respiratory Disease Complex. J Vet Intern Med [Internet]. 2015;29(3):770–80. Available from: http://onlinelibrary.wiley.com/doi/10.1111/jvim.12597/full
8. Buczinski S, L Ollivett T, Dendukuri N. Bayesian estimation of the accuracy of the calf respiratory scoring chart and ultrasonography for the diagnosis of bovine respiratory disease in pre-weaned dairy calves. Prev Vet Med. 2015;
9. Schaffer AP, Larson RL, Cernicchiaro N, Hanzlicek GA, Bartle SJ, Thomson DU. The association between calfhood bovine respiratory disease complex and subsequent departure from the herd, milk production, and reproduction in dairy cattle. J Am Vet Med Assoc. 2016;248(10):1157–64.
10. Houghton, S. B. and RNG. Synergism between Mycoplasma bovis and Pasteurella haemolytica in calf pneumonia. Vet Rec. 1983;113(2):41–2.
11. Hodgins DC, Conlon JA SP. Respiratory Viruses and Bacteria in Cattle. In: Brogden KA GJ, editor. Polymicrobial Diseases. Washington (DC): ASM Press; 2002.
12. Taylor JD, Fulton RW, Lehenbauer TW, Step DL, Confer AW. The epidemiology of bovine respiratory disease: What is the evidence for preventive measures? Can Vet J. 2010;51:1351–9.
13. USDA:APHIS:VS. Dairy 2007 Part V: Changes in Dairy Cattle Health and Management Practices in the United States, 1996-2007. United States Dept Agric [Internet]. 2009;(February):N512-1008. Available from: http://scholar.google.com/scholar?hl=en&btnG=Search&q=intitle:Beef+2007-08+Part+1:+Reference+of+Beef+Cow-calf+Management+Practices+in+the+United+States,+2007-08#9
14. Ward H, Powell J. Livestock health series: Bovine respiratory disease [Internet]. Div. Agric. Fact Sheet FSA3082. Fayetteville, AR; 2013. Available from: http://www.uaex.edu/publications/pdf/FSA- 3082.pdf
15. Brooks K, Raper K, Ward C. Economic effects of bovine respiratory disease on feedlot cattle during backgrounding and finishing phases. Prof … [Internet].

2011;27:195–203. Available from: http://pas.fass.org/content/27/3/195.short
16. Wittum TE, Woollen NE, Perino LJ, Littledike ET. Relationships among treatment for respiratory tract disease, pulmonary lesions evident at slaughter, and rate of weight gain in feedlot cattle. J Am Vet Med Assoc [Internet]. 1996;209(4):814–8. Available from: http://www.ncbi.nlm.nih.gov/pubmed/8756886
17. Epling GP. Electron microscopy of the bovine lungs: the blood-air barrier in acute pulmonary emphysema. Am J Vet Res. 1964;(1431–1445).
18. Adams EA, Buczinski S. Short communication: Ultrasonographic assessment of lung consolidation postweaning and survival to the first lactation in dairy heifers. J Dairy Sci. 2016;99(2):1465–70.
19. Bach A. Associations between several aspects of heifer development and dairy cow survivability to second lactation. J Dairy Sci. 2011;94(2):1052–7.
20. Budras, Klaus Dieter; Habel, Robert E.; Mülling, Christoph K. W.; Greenough, Paul R.; Jahrmärker, Gisela; Richter, Renate; Starke D. Bovine Anatomy: An Illustrated Text. 2nd ed. Hanover, Germany: Schluetersche; 2011. 62-63 p.
21. Tyler WS. Small Airways and Terminal Units Comparative Subgross Anatomy of Lungs Pleuras, Interlobular Septa, and Distal Airways. Am Rev Respir Dis [Internet]. 1983;128(2 Pt 2):S32-6. Available from: http://www.ncbi.nlm.nih.gov/pubmed/6881704
22. Veit HP, Farrell RL. The anatomy and physiology of the bovine respiratory system relating to pulmonary disease. Cornell Vet. 1978;68:555–81.
23. Bradbury S. Respiratory System. In: Hewer's textbook of histology for Medical Students. 9th ed. London, England: Heinemann Medical Books; 1973. p. 258–73.
24. Peake, Janice L.; Pinkerton KE. Gross and Subgross Anatomy of Lungs, Pleura, Connective Tissue Septa, Distal Airways, and Structural Units. In: Parent R, editor. Comparative Biology of the Normal Lung. 2nd ed. Academic Press, Elsevier; 2015. p. 21–31.
25. Leong, F. J. W. M., Eum, S., Via, L. E., & Barry 3rd CE. Pathology of tuberculosis in the human lung. In: A Color Atlas of Comparative Pathology of Pulmonary Tuberculosis. 2011. p. 53–81.
26. Stamp JT. The distribution of the bronchial tree in the bovine lung. J Comp Pathol Ther. 1948;58:1–8.
27. Budras, Klaus Dieter; McCarthy, Patrick H.; Berg, Rolf; Horowitz A. Anatomy of the Dog: An Illustrated Text. 5th ed. Hanover, Germany: Schluetersche; 2007. 38-42 p.
28. Griffin D. The monster we don't see: subclinical BRD in beef cattle. Anim Heal Res Rev. 2014;15(2):138–41.
29. Thomas LH, Scott EJ, Collins AP, Jebbett NJ, Stark AJ. Evaluation of respiratory disease in calves: comparison of disease response to different viruses. Res Vet Sci. 1977;23:157–64.
30. McGuirk SM, Peek SF, McGuirk , Sheila M.; Peek SF, McGuirk SM, Peek SF. Timely diagnosis of dairy calf respiratory disease using a standardized scoring system. Anim Heal Res Rev. 2014;15(2):145–7.
31. Wolfger B, Timsit E, White BJ, Orsel K. A Systematic Review of Bovine Respiratory Disease Diagnosis Focused on Diagnostic Confirmation, Early

Detection, and Prediction of Unfavorable Outcomes in Feedlot Cattle. Vet Clin North Am Food Anim Pract [Internet]. 2015 Nov;31(3):351–65. Available from: http://www.sciencedirect.com/science/article/pii/S0749072015000419
32. Severidt JA, Madden DJ, Mason G, Garry F, Gould D. Dairy Cattle Necropsy Manual [Internet]. 2002 [cited 2017 May 10]. Available from: https://www.cvmbs.colostate.edu/ilm/proinfo/necropsy/notes/index.html
33. England JJ, Anderson BC. Evaluating Dead Cattle: A Necropsy Guide for the Cow-Calf Operation [Internet]. Cattle Producer's Handbook 3rd Edition. 2012 [cited 2017 May 15]. p. 603. Available from: http://blogs.oregonstate.edu/beefcattle/files/2016/09/603-Evaluating-Dead-Cattle-A-Necropsy-Guide-for-the-Cow-Calf-Operation.pdf
34. Turner GDH, Bunthi C, Wonodi CB, Morpeth SC, Molyneux CS, Zaki SR, et al. The role of postmortem studies in Pneumonia etiology research. Clin Infect Dis. 2012;54(SUPPL. 2):S165–71.
35. King JM, Roth-Johnson L, Dodd DC, Newsom ME. THE NECROPSY BOOK: A Guide for Veterinary Students, Residents, Clinicians, Pathologists, and Biological Researchers. 2014;(October 2014).
36. Anspaugh D, Th DU, Wileman B, Apley M, Taylor W, No T, et al. Agreement Between Observational and Necropsy-Derived Diagnosis for Cause of Death for Cattle in a Commercial Beef Feedlot. 2009;8–11.
37. Ollivett T. Understanding the Diagnosis and Risk Factors for Respiratory Disease in Dairy Calves. 2014.
38. McGuirk SM. Disease Management of Dairy Calves and Heifers. Vet Clin North Am - Food Anim Pract. 2008;24(1):139–53.
39. SG. N. The equine thorax. In: DE T, editor. Textbook of veterinary diagnostic radiology. 6th ed. St. Louis, MO: Elsevier; 2013. p. 632–49.
40. Verschooten, F., W. Oyaert and RD. Radiographic diagnosis of lung diseases in cattle. Vet Radiol Ultrasound. 1974;15(1):49–59.
41. Bargai, Uri; Pharr, John W.; Morgan JP. Bovine radiology. Iowa State University Press; 1989.
42. Corradi F, Brusasco C, Garlaschi A, Paparo F, Ball L, Santori G, et al. Quantitative analysis of lung ultrasonography for the detection of community-acquired pneumonia: A pilot study. Biomed Res Int. 2015;1–8.
43. Syrjala H, Broas M, Suramo I, Ojala A, La S. High-Resolution Computed Tomography for the Diagnosis of Community-. Clin Infect Dis. 1998;27(2):358–63.
44. Farrow CS. Bovine pneumonia. Its radiographic appearance. Vet Clin North Am Food Anim Pract. 1999;15(2):301–58, vi–vii.
45. Lee R. Bovine Respiratory Disease : Its Radiological Features. Vet Radiol Ultrasound. 1973;15(1):41–7.
46. Tyson R, Smiley DC, Pleasant RS, Daniel GB. Estimated operator exposure for hand holding portable x-ray units during imaging of the equine distal extremity. Vet Radiol Ultrasound. 2011;52(2):121–4.
47. Ackerman N, Spencer CP, Hager DA, Poulos PW. Radiation Exposure During Equine Radiography. Vet Radiol. 1988;29(5):198–201.

48. Lynch T, Bialy L, Kellner JD, Osmond MH, Klassen TP, Durec T, et al. A systematic review on the diagnosis of pediatric bacterial pneumonia: When gold is bronze. PLoS One. 2010;5(8).
49. Rizzi EB, Schinina' V, Cristofaro M, Goletti D, Palmieri F, Bevilacqua N, et al. Detection of Pulmonary tuberculosis: comparing MR imaging with HRCT. BMC Infect Dis [Internet]. 2011;11:243. Available from: http://www.pubmedcentral.nih.gov/articlerender.fcgi?artid=3184086&tool=pmcentrez&rendertype=abstract
50. Prather AB, Berry CR, Thrall DE. Use of radiography in combination with computed tomography for the assessment of noncardiac thoracic disease in the dog and cat. Vet Radiol Ultrasound. 2005;46(2):114–21.
51. Worthy S. High resolution computed tomography of the lungs. BMJ. 1995;310:616.
52. Bessis L, Callard P, Gotheil C, Biaggi A, Grenier P. High-resolution CT of parenchymal lung disease: precise correlation with histologic findings. Radiographics [Internet]. 1992;12(1):45–58. Available from: http://www.ncbi.nlm.nih.gov/entrez/query.fcgi?cmd=Retrieve&db=PubMed&dopt=Citation&list_uids=1734481
53. Jones JC, Wilson ME, Bartels JE. A review of high resolution computed tomography and a proposed technique for regional examination of the canine lumbosacral spine. Vet Radiol Ultrasound. 1994;35(5):339–46.
54. Lascola KM, O'Brien RT, Wilkins PA, Clark-Price SC, Hartman SK, Mitchell MA. Qualitative and quantitative interpretation of computed tomography of the lungs in healthy neonatal foals. Am J Vet Res. 2013;74(9):1239–46.
55. Ohlerth S, Augsburger H, Abe M, Ringer S, Hatz L, Braun U. Computed tomography of the thorax in calves from birth to 105 days of age. Schweiz Arch Tierheilkd. 2014;156(10):489–97.
56. Tsuka T, Yamamoto N, Saneshige M, Morita T, Sunden Y, Murahata Y, et al. Computed tomographic images of discospondylitis in a calf. J Vet Med Sci. 2015;77(12):1689–91.
57. Becker M, Heun C, Tsousis G, Bollwein H. Application of computed tomography for the evaluation of obstetrically relevant measurements in German Holstein-Friesian calves. Theriogenology. 2011;
58. Finnen A, Blond L, Francoz D, Parent J. Comparison of Computed Tomography and Routine Radiography of the Tympanic Bullae in the Diagnosis of Otitis Media in the Calf. J Vet Intern Med. 2011;25(1):143–7.
59. Henao-Guerrero N, Ricco C, Jones JC, Buechner-Maxwell V, Daniel GB. Comparison of 4 ventilatory protocols for CT of the thorax in healthy cats. Am J Vet Res. 2012;73(5):646–53.
60. Saklad M. Grading of patients for surgical procedures. Anesthesiology. 1941;2:281–4.
61. No Title [Internet]. American Society of Anesthesiologists (ASA) Physical Status Scale. [cited 2017 Apr 4]. Available from: http://www.avtaa-vts.org/asa-ratings.pml
62. Stadler K, O'Brien R. Computed tomography of nonanesthetized cats with upper

airway obstruction. Vet Radiol Ultrasound. 2013;54(3).
63. Oliveira CR, Mitchell MA, O'Brien RT. Thoracic computed tomography in feline patients without use of chemical restraint. Vet Radiol Ultrasound. 2011;52(4):368–76.
64. Stadler K, Hartman S, Matheson J, O'Brien R. Computed tomographic imaging of dogs with primary laryngeal or tracheal airway obstruction. Vet Radiol Ultrasound. 2011;
65. Shanaman MM, Hartman SK, O'Brien RT. Feasibility for using dual-phase contrast-enhanced multi-detector helical computed tomography to evaluate awake and sedated dogs with acute abdominal signs. Vet Radiol Ultrasound. 2012;53(6):605–12.
66. Lee K, Heng HG, Jeong J, Naughton JF, Rohleder JJ. Feasibility of computed tomography in awake dogs with traumatic pelvic fracture. Vet Radiol Ultrasound. 2012;53(4):412–6.
67. Lubbers B V., Apley MD, Coetzee JF, Mosier DA, Biller DS, Mason DE, et al. Use of computed tomography to evaluate pathologic changes in the lungs of calves with experimentally induced respiratory tract disease. Am J Vet Res. 2007;68(11):1259–64.
68. Hansell DM, Bankier AA, MacMahon H, McLoud TC, Müller NL, Remy J. Fleischner Society: glossary of terms for thoracic imaging. Radiology [Internet]. 2008;246(3):697–722. Available from: http://pubs.rsna.org/doi/full/10.1148/radiol.2462070712
69. Schliewert EC, Lascola KM, O'Brien RT, Clark-Price SC, Wilkins PA, Foreman JH, et al. Comparison of radiographic and computed tomographic images of the lungs in healthy neonatal foals. Am J Vet Res. 2015;
70. Mesquita L, Lam R, Lamb CR, Mcconnell JF. Computed tomographic findings in 15 dogs with eosinophilic bronchopneumopathy. Vet Radiol Ultrasound. 2015;56(1):33–9.
71. Thierry F, Handel I, Hammond G, King LG, Corcoran BM, Schwarz T, et al. Further characterization of computed tomographic and clinical features for staging and prognosis of idiopathic pulmonary fibrosis in West Highland white terriers. Vet Radiol Ultrasounddi. 2017;(October 2016):1–8.
72. Dennler M, Makara M, Kranjc A, Schnyder M, Ossent P, Deplazes P, et al. Thoracic computed tomography findings in dogs experimentally infected with angiostrongylus vasorum. Vet Radiol Ultrasound. 2011;
73. Fina C, Vignoli M, Terragni R, Rossi F, Wisner E, Saunders JH. Computed tomographic characteristics of eosinophilic pulmonary granulomatosis in five dogs. Vet Radiol Ultrasound. 2014;55(1):16–22.
74. Schwarz, Tobias; Johnson V. Lungs and Bronchi. In: Schwarz, Tobias; Saunders J, editor. Veterinary Computed Tomography. West Sussex, UK: Wiley-Blackwell; 2011. p. 261–77.
75. Reali F, Sferrazza Papa GF, Carlucci P, Fracasso P, Di Marco F, Mandelli M, et al. Can lung ultrasound replace chest radiography for the diagnosis of pneumonia in hospitalized children? Respiration. 2014;
76. Boysen SR, Lisciandro GR. The use of ultrasound for dogs and cats in the

emergency room AFAST and TFAST. Veterinary Clinics of North America - Small Animal Practice. 2013.
77. Jung, C. and Bostedt H. Thoracic Ultrasonography Technique in Newborn Calves and Description of Normal and Pathological Findings. Vet Radiol Ultrasound. 2004;45:331–5.
78. Volpicelli G, Elbarbary M, Blaivas M, Lichtenstein DA, Mathis G, Kirkpatrick AW, et al. International evidence-based recommendations for point-of-care lung ultrasound. In: Intensive Care Medicine. 2012.
79. Lichtenstein D. Lung ultrasound in the critically ill. Curr Opin Crit Care [Internet]. 2014;20(3):315–22. Available from: http://content.wkhealth.com/linkback/openurl?sid=WKPTLP:landingpage&an=00075198-201406000-00015
80. Feldman MK, Katyal S, Blackwood MS. US Artifacts. RadioGraphics [Internet]. Radiological Society of North America; 2009 Jul 1;29(4):1179–89. Available from: http://dx.doi.org/10.1148/rg.294085199
81. Gibikote S, Verghese VP. Diagnosis of pneumonia in children- ultrasound better than cxr. Radiol Medica. 2008;113(7):1079–80.
82. Llamas-Álvarez AM, Tenza-Lozano EM, Latour-Pérez J. Accuracy of lung ultrasound in the diagnosis of pneumonia in adults: systematic review and meta-analysis. Chest [Internet]. 2016; Available from: http://dx.doi.org/10.1016/j.chest.2016.10.039
83. Fields EL, Robertson ID, Osborne JA, Brown JC. Comparison of abdominal computed tomography and abdominal ultrasound in sedated dogs. Vet Radiol Ultrasound. 2012;53(5):513–7.
84. Adrian AM, Barrett MF, Werpy NM, Kawcak CE, Chapman PL, Goodrich LR. A comparison of arthroscopy to ultrasonography for identification of pathology of the equine stifle. Equine Vet J. 2016;49:314–21.
85. Pinto A, Pinto F, Faggian A, Rubini G, Caranci F, Macarini L, et al. Sources of error in emergency ultrasonography. Crit Ultrasound J [Internet]. Springer; 2013 Jul 15;5(Suppl 1):S1–S1. Available from: http://www.ncbi.nlm.nih.gov/pmc/articles/PMC3711733/
86. Caiulo VA, Gargani L, Caiulo S, Fisicaro A, Moramarco F, Latini G, et al. Lung ultrasound in bronchiolitis: Comparison with chest X-ray. Eur J Pediatr. 2011;170(11):1427–33.
87. Sperandeo M, Varriale A, Sperandeo G, Filabozzi P, Piattelli ML, Carnevale V, et al. Transthoracic ultrasound in the evaluation of pulmonary fibrosis: our experience. Ultrasound Med Biol. 2009;35(5):723–9.
88. Zieleskiewicz L, Lagier D, Contargyris C, Bourgoin A, Gavage L, Martin C, et al. Lung ultrasound-guided management of acute breathlessness during pregnancy. Anaesthesia. 2013;68(1):97–101.
89. Rademacher N, Pariaut R, Pate J, Saelinger C, Kearney MT, Gaschen L. Transthoracic lung ultrasound in normal dogs and dogs with cardiogenic pulmonary edema: A pilot study. Vet Radiol Ultrasound. 2014;55(4):447–52.
90. Vezzosi T, Mannucci T, Pistoresi A, Toma F, Tognetti R, Zini E, et al. Assessment of Lung Ultrasound B-Lines in Dogs with Different Stages of Chronic Valvular

Heart Disease. J Vet Intern Med [Internet]. 2017;17–9. Available from: http://doi.wiley.com/10.1111/jvim.14692
91. Ward JL, Lisciandro GR, Keene BW, Tou SP DT. Accuracy of point-of-care lung ultrasonography for the diagnosis of cardiogenic pulmonary edema in dogs and cats with acute dyspnea. J Am Vet Med Assoc. 2017;250(6):666–75.
92. Ollivett TL, Caswell JL, Nydam D V., Duffield T, Leslie KE, Hewson J, et al. Thoracic Ultrasonography and Bronchoalveolar Lavage Fluid Analysis in Holstein Calves with Subclinical Lung Lesions. J Vet Intern Med. 2015;29(6):1728–34.
93. Buczinski, S., Forté, G., Francoz, D., & Bélanger AM. Comparison of thoracic auscultation, clinical score, and ultrasonography as indicators of bovine respiratory disease in preweaned dairy calves. J Vet Intern Med. 2014;28(1):234–42.
94. Rabeling B, Rehage J, Dopfer D, Scholz H. Ultrasonographic findings in calves with respiratory disease. 1998;
95. Abutarbush SM, Pollock CM, Wildman BK, Perrett T, Schunicht OC, Kent Fenton R, et al. Evaluation of the diagnostic and prognostic utility of ultrasonography at first diagnosis of presumptive bovine respiratory disease. Artic Can J Vet Res. 2012;76(23):23–32.

Chapter 2- Scope of the Study

Thoracic imaging of calves with respiratory disease is commonly performed using thoracic ultrasound (US), but scant data are available determining the diagnostic accuracy of thoracic imaging. Additionally, of the studies currently available, most were completed utilizing calves with experimentally induced pulmonary disease. Given the prevalence of respiratory disease in juvenile dairy cattle and the increasing availability of portable US for use as an on-farm diagnostic tool, further knowledge is necessary to better assess the use of US in evaluation of the presence of pulmonary disease.

The objective of the first study was to evaluate the severity and extent of lung disease using thoracic computed radiography (CR) compared to contrast-enhanced multi-detector computed tomography (MDCT) of the thorax in calves with naturally acquired respiratory disease and to evaluate the feasibility and safety of performing contrast enhanced MDCT examinations in sedated calves. We hypothesized, that thoracic CR would be sufficient to diagnose lung disease in calves; but that MDCT in sedated calves could be safely performed and would provide more information about the extent of lung involvement. Furthermore, to evaluate if combining CR or CT with respiratory scoring factors will improve prediction of the chronicity of pulmonary disease in calves. The first study is presented in Chapter 3, and the knowledge obtained in the first study was utilized to guide the study design for the second study.

The objective of the second study was to assess the accuracy of imaging findings suggestive of pneumonia using thoracic radiography, computed tomography and pulmonary ultrasound in comparison to histopathology and clinical disease scoring using the Wisconsin method in calves with naturally acquired respiratory disease and healthy

calves. We hypothesized that the diagnostic accuracy of ultrasound for identifying and localizing pneumonia is similar to thoracic radiography and computed tomography. Additionally, we hypothesized that thoracic imaging, regardless of modality, would be more sensitive than clinical respiratory scoring via the Wisconsin method for diagnosing pneumonia in calves. The second study is presented in Chapter 4.

Comparison of Thoracic Radiography and Computed Tomography in Calves with Naturally Occurring Respiratory Disease

Jennifer L Fowler, Susanne M Stieger-Vanegas, Jorge A Vanegas, Gerd Bobe, and Keith P Poulsen

A manuscript published by:
Frontiers in Veterinary Science
http://journal.frontiersin.org/article/10.3389/fvets.2017.00101/full
2017, Issue 4, article 101, doi: 10.3389/fvets.2017.00101

Chapter 3- Comparison of Thoracic Radiography and Computed Tomography in Calves with Naturally Occurring Respiratory Disease

3.1 Introduction

Respiratory disease in cattle is the most prevalent cause of morbidity and mortality in beef feedlots, and the most common cause of morbidity in weaned dairy calves.(1) Early diagnosis of disease is essential to reduce the risk of disease propagation and to decrease the financial costs from treatment and loss of animals. Furthermore, early diagnosis promotes good quality of life for the patient, improves response to treatment, and decreases the likelihood of prolonged morbidity following juvenile pneumonias.(2,3)

Calves with respiratory disease often present with fever, cough and tachypnea. Auscultation is commonly used to further evaluate the lungs. However, several of these clinical findings have been proven unreliable to diagnose pneumonia in calves. As such, diagnosis of bovine respiratory disease remains a diagnostic challenge.

Thoracic radiography is the most commonly used test of choice to evaluate for pneumonia in human and veterinary patients. Radiography of the thorax of large animals can be limited to having only lateral projections of the thorax available for interpretation and by inadequate penetration due to the size of large animals and equipment limitations; however its practicality including its use in field conditions, low cost and widespread availability make it one of the most common used techniques to evaluate the thorax in large animals with respiratory disease.(4–6) Computed tomography (CT) of the thorax is considered the modality of choice to evaluate for the presence of lung disease in human patients and is increasingly used in veterinary patients.(7) Thoracic CT has proven to be

helpful for evaluating the extent of pulmonary disease and provides better anatomic detail due to a lack of superimposition of anatomical structures.(8) The use of CT in calves is often limited by the cost and lack of availability of a CT scanner close to a calf rearing operation. Furthermore, CT examinations of the thorax are commonly performed under general anesthesia with endotracheal intubation to allow using breath-hold techniques, which decrease the risk of respiratory motion.(9,10) However, calves with severe respiratory impairment due to pneumonia often have an increased anesthetic risk. Although CT scanning protocols have been described for awake and sedated patients including for normal cats,(11) cats with upper airway obstruction and intrathoracic disease,(12) dogs with acute abdominal signs,(13) and dogs with traumatic pelvic fractures,(14) healthy sedated foals,(15) neither has been evaluated in calves to date.

Our objective was to compare the severity and extent of lung disease using computed radiography (CR) compared to contrast-enhanced multidetector CT (MDCT) of the thorax and further determine the feasibility and safety of performing thoracic MDCT examinations in sedated calves with naturally occurring respiratory disease. We hypothesized that thoracic CR would be sufficient to diagnose lung disease in calves; but that MDCT in sedated calves could be safely performed and would provide more information about the extent of lung involvement. We further wanted to evaluate if combining CR or MDCT with respiratory scoring factors will improve prediction of the chronicity of pulmonary disease in calves.

3.2 Materials and Methods

3.2.1 Study Population

Thirty privately owned pre-weaned Jersey heifer calves with naturally occurring respiratory disease ranging in age between 25 - 89 days (50.5 ± 18.8 days) were included in the study. The calves with respiratory disease were identified by farm workers dedicated to calf health monitoring and treatment using a clinical respiratory disease scoring system.(16) On the farm, the calves were grouped based on respiratory disease duration into acute disease (within 24 hour of first signs of clinical pulmonary disease, group 1) and chronic disease. Calves with chronic pulmonary disease had received antibiotic treatment at the onset of clinical pulmonary disease but continued to exhibit clinical signs of pneumonia. Chronic disease calves were subdivided into two groups: group 2 included calves which had received one antibiotic treatment 1 week prior (short-term chronic disease), and group 3 included calves which had received antibiotic treatments 2 weeks and 1 week prior (long-term chronic disease).

To study the effect of naturally occurring respiratory disease duration on imaging findings out of each group (acute, short-term and long-term chronic) ten calves were randomly selected and transported to the Lois Bates Acheson Veterinary Teaching Hospital at Oregon State University for the imaging studies. Calves were housed with free choice of water, calf starter, and were fed milk replacer twice daily until the imaging studies were performed. All imaging studies were performed within 24-48 hours post respiratory scoring on the farm. The study was approved by the Oregon State University Institutional Animal Care and Use Committee.

3.2.2 Thoracic Computed Radiography

Standing left to right lateral computed radiography[a] images of the thorax were obtained using 85kVp and 20 to 32 mAs at 630 mA. If calves were smaller in size, the exposure was adjusted by reducing the mAs to 20 and keeping the mA constant at 630 to ensure optimal image quality. One or up to three radiographs of the thorax were obtained to ensure that all aspects of the lungs were included in the study. All diagnostic images were sent to a designated image storage server for off-line analysis.

3.2.3 Multi-Detector Computed Tomography

All thoracic CT studies were performed under sedation using a 64-row mulitdetector CT scanner (MDCT)[b]. Prior to the MDCT study a jugular vein catheter was aseptically placed in each calf. Calves were sedated with a combination of 0.1 mg/kg butorphanol[c], 0.3 mg/kg ketamine[d], and 0.4 mg/kg xylazine[e] for the MDCT study. All thoracic MDCT scans were performed with the calves positioned in sternal recumbency. A non-contrast enhanced thoracic MDCT scan followed by a contrast enhanced MDCT scan was performed in each calf from approximately 10 cm cranial to the thoracic inlet to the mid-level of the left kidney using the following scan parameters: 0.5 mm collimation, 0.5 mm reconstruction interval, 1 sec tube rotation time, 120 kV, 400 mA, a pitch factor of 0.828, and 0-degree tilt. The contrast-enhanced MDCT scan was performed 60 s after the start of an intravenous iodinated contrast agent[f] injection at 1 mL/kg using a power injector [g] at a flow rate of 3 mL/s. The thin collimated MDCT isovolumetric data were used to create transverse, sagittal and dorsal reconstructed images of the thorax with 3 mm slice thickness. A bone, soft tissue and lung algorithm was used to create bone, soft tissue and lung window images. Images were sent to a designated image storage server

for later analysis. Following MDCT imaging, the calves were humanely euthanatized with intravenous pentobarbital [h] at 0.2 ml/kg in accordance with the American Veterinary Medical Association guidelines.

3.2.4 Image Evaluation

All diagnostic imaging studies were evaluated independently by two evaluators (JF, SSV) using a commercially available DICOM viewer software[i]. Each thoracic CR and MDCT study of each calf was evaluated independently and separately by each evaluator. Both evaluators were blinded to the group assignment of the calves and the results of each imaging study. The CR and MDCT studies were evaluated for diagnostic quality and graded as poor, acceptable and excellent. The imaging studies were graded as excellent if no motion artifacts were present, as acceptable if motion was present to a degree that did not hinder evaluation of the lung parenchyma and pleural surface, or as poor if the study had to be repeated due to extensive motion causing a non-diagnostic study.

Additionally, on CT images the maximum height and length of the right and left lung were measured as well as the maximum tracheal diameter in the mid thorax and at the level just cranial of the tracheal bifurcation. Furthermore, the attenuation of the lung parenchyma was measured in pre- and post-contrast agent injection images at the ventral, mid and dorsal levels by drawing a circular region of interest (ROI) of 0.3 cm in diameter encompassing lung parenchyma at each level and intercostal space to measure the average Hounsfield units (HU) in this drawn area. Pre- and post-contrast agent injection images were lined up with each other, so that measurements were made in the same anatomic area. No larger vessels or bronchi were included in the ROIs.

For evaluation of the lung in each imaging modality, the thorax was divided in four quadrants (Fig. 3-1). The quadrants were defined by a horizontal line running parallel to and at the level of the ventral tracheal margin for a dorsal-ventral delineation, and by a vertical line at the level of and parallel to the caudal margin of the fifth rib for a cranial-caudal delineation. The resulting quadrants of the thorax were craniodorsal (CrD), cranioventral (CrV), caudodorsal (CdD) and caudoventral (CdV).

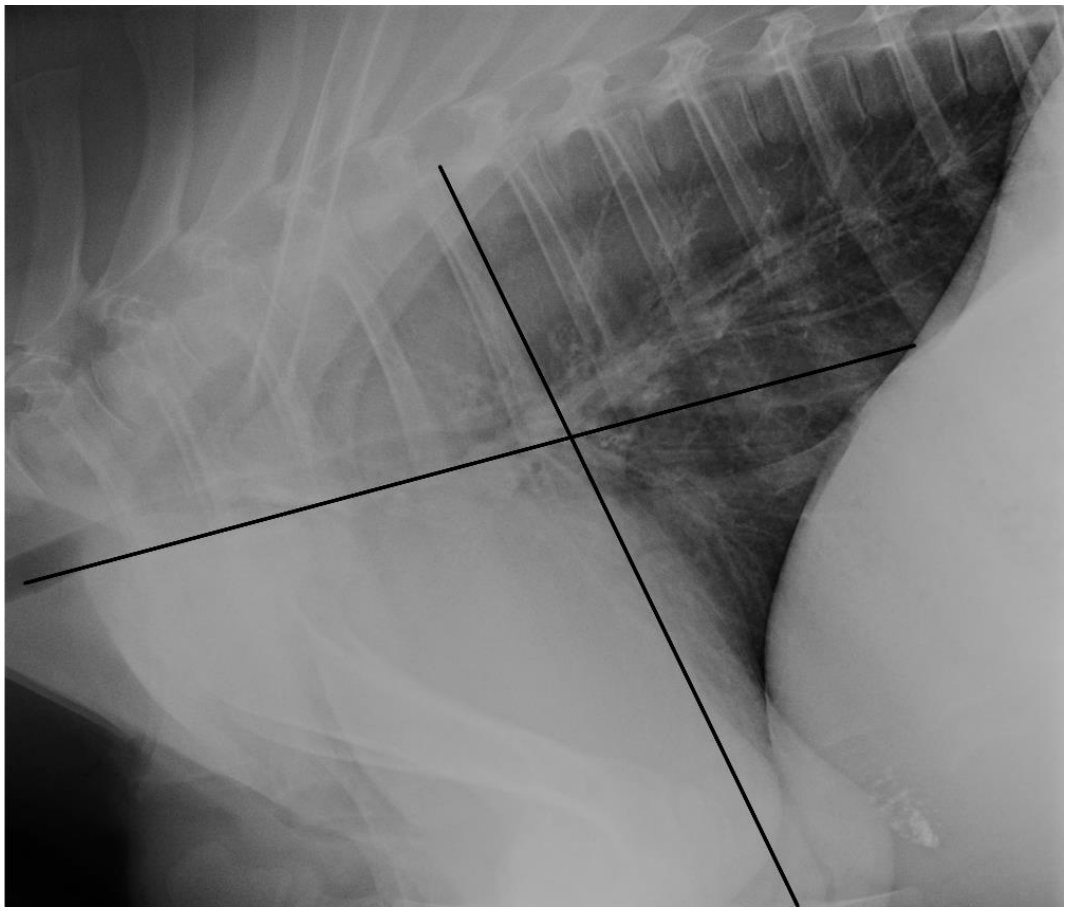

Figure 3-1 Division of the thorax into four quadrants for pulmonary pattern and severity identification is illustrated on a lateral radiograph of the thorax of a 69-day old Jersey heifer calf. The line parallel with the ventral aspect of the trachea divides the thorax into a dorsal and ventral half. The line parallel with the caudal border of the 5th rib divides the thorax into a cranial and caudal half.

Within each quadrant, alterations of the lung parenchyma and airways were assessed by describing the predominant abnormal pulmonary pattern using the following criteria: presence of prominent and/or thickened bronchial walls (bronchial), a diffuse increased opacity of the lung parenchyma causing loss of definition of the vascular structures (unstructured interstitial), a soft tissue opacity of the lung with the presence of air bronchograms (alveolar with air bronchograms) completely obscuring identification of the vascular structures, borders of the heart or diaphragm, a focal soft tissue opacity in the lung without the presence of air bronchograms (alveolar without air bronchograms), which is completely obscuring identification of other structures. The presence of one or more soft tissue opacity structures measuring up to 3 cm in diameter (nodular), and no abnormality of the pulmonary parenchyma was noted (normal).

In each quadrant of the thorax, an estimate of the percentage of abnormal lung parenchyma was made based on the presence of any pathologic pattern being identified regardless of severity. For example, if 50% of a region was abnormal due to an unstructured interstitial pattern and 50% due to an alveolar pattern with air bronchograms, then this region would be listed as 100% abnormal. If an entire region of lung was considered normal, the region was labeled as 0% to indicate absence of disease.

Furthermore, the presence of pleural fluid was recorded as a yes/no result. The degree of pleural fluid was noted as: within the limits of the ventral third of the thorax (mild), within the limits of the mid third of the thorax (moderate), and extending to the dorsal third of the thorax (severe).

Additionally, the presence of visceral and parietal pleural thickening was recorded as a yes/no answer. The degree of pleural thickening was graded as: less than three focal

areas of thickening noted (mild), between 4-6 areas of focal pleural thickening noted (moderate), and more than 7 areas of focal pleural thickening noted (severe).

3.2.5 Pathology and Microbiology

Prior to gross necropsy, nasopharyngeal swabs were collected in each calf for *Mycoplasma* culture and speciation, and *M. bovis* polymerase chain reaction (PCR). During necropsy, lung tissue was collected from various lung regions and submitted for *Mycoplasma* culture and speciation, *M. bovis* PCR, and aerobic bacterial culture and sensitivity. Bacteriology and molecular biology diagnostic evaluations were performed at the Oregon State Veterinary Diagnostic Laboratory (Corvallis, OR). *Mycoplasma* speciation was performed by fluorescent antibody microscopy at the Wisconsin Veterinary Diagnostic Laboratory (Madison, WI). Samples of all major organ tissues were harvested for histopathology.

3.2.6 Statistical Analysis

Statistical analysis was performed with commercial software [k]. Quantitative data were assessed for normality using the Kolmogorov-Smirnov normality test and reported as mean ± standard deviation when normally distributed and as median and range when not. For comparisons between disease groups, quantitative, normal distributed data were analyzed using a one-way ANOVA with Sidak's multiple comparisons test adjustment for group differences, not normal-distributed quantitative data were analyzed using Wilcoxon rank sum test, and binary data were analyzed using Fisher's exact test.

For comparisons of imaging modalities within calf, comparisons of lung quarters within the same calf, and for comparison of evaluators within the same calf, multinomial

categorical data were analyzed using a Wilcoxon matched pairs signed rank test and binary paired data were analyzed using McNemar's test. Categorical data with more than two categories (i.e., disease stage) were collapsed to binary data, if one category dominated the other categories. Inter- and intra-observer agreements were calculated of multinomial categorical data and statistically analyzed using kappa statistics. Statistical significance was set at $p < 0.05$.

3.3 Results

3.3.1 Animals

Calves in the first-time diagnosis group (group 1) and the short-term chronic group (group 2) were similar in age (40.7 ± 16.2 days versus 47.3 ± 13.9 days) and respiratory scores (group 1- 9.6±1.5, range: 7-12; group 2- 8.3±1.6, range 5-11). Calves in the long-term chronic group (group 3) were older than calves in group 1 and 2 (63.4 ± 19.3 days) and had statistically lower respiratory scores than group 1 (7.6 ± 1.8, range: 4-11; p=0.03). Of the respiratory score criteria, only body temperature differed between groups 1 and 3 (group 1- 40.1 ± 0.4 C, group 3- 38.7 ± 0.7 C; p<0.0001). All group 1 calves had a body temperature of 39.5 C or greater, whereas only 3 calves in group 2 and 1 calf in group 3 had a body temperature of 39.5 C or greater.

All 30 calves selected for inclusion in the study survived the imaging procedures without the need for additional medical care or sedation reversal agents.

3.3.2 Thoracic Computed Radiography

All, but one radiographic study was performed with the calves standing. One calf was unwilling to stand, so the calf was positioned sternally with the forelimbs extended

cranially and left-to-right lateral radiographs of the thorax were obtained. Two radiographs of the thorax were sufficient in all calves to ensure that the entire thorax was included within image collimation. All radiographic images were of acceptable to excellent quality and no repeat radiographic studies were required.

3.3.3 Thoracic Multi-Detector Computed Tomography

Pre-contrast studies were obtained in 100% of patients. Of the survey scans, all were deemed suitable for evaluation by both evaluators, without a marked degree of motion artifact to cause inhibition of pulmonary parenchyma evaluation.

Of the pre-contrast studies, 8/30 (26.7%) cases had negligible motion artifact, 17/30 (56.7%) cases had a mild amount of motion artifact causing mild loss of distinction of the margins of the tertiary bronchi, and 5/30 (16.6%) cases had a moderate amount of motion artifact causing complete loss of distinction of the tertiary bronchi and a mild loss of definition of the larger secondary bronchi. No pre-contrast studies had marked motion artifact.

Intravenous contrast medium administration failed for one case, in which the jugular vein catheter displaced when moving the animal and the contrast medium leaked into the perivascular space of the neck. Post-contrast images were successfully obtained in 97% of cases (29/30). Of the 29 cases in which post-contrast images were available for evaluation, all MDCT scans were deemed suitable for evaluation.

All studies had some degree of respiratory motion induced slice mismatch between the pre- and post-contrast medium administration acquisitions. All post-contrast medium administration studies had a respiratory motion artifact, with 21/30 (70%) having mild motion, and 8/30 (26.7%) having moderate motion artifact. A marked amount of

respiratory motion artifact was seen in 1/30 (3.3%); however, the severity of the artifact was not to the degree that it would prevent diagnostic assessment of the images. In the case of extravasation of contrast medium from the jugular vein, the degree of motion artifact was unchanged between the pre- and post-contrast medium administration images.

The cranial border of the cranial lungs was at the level of the first rib in all but one calf, in which the lung extended mildly cranial to the first rib. The caudal border of the lungs ranged from the level of the 11^{th} to 13^{th} rib (average 12.0 ± 0.7). The length and height of the right and left lungs as well as the tracheal diameter were not significantly different in any of the groups. The differences were less than 1.1 cm in right and left lung height and length, and less than 0.1 cm in the tracheal diameter between the three groups.

The lung parenchymal attenuation averaged throughout all lung lobes before and after intravenous iodinated contrast agent injection was not statistically different between the groups (Table 3-1).

The average of contrast enhancement throughout all lung lobes was not statistically different between the groups and averaged in group 1= 32.7 HU, in group 2 = 24.6 HU and in group 3 – 30.4 HU. The maximum difference between before and after intravenous iodinated contrast agent injection images averaged 54.3 HU in group 1, 49.3 HU in group 2 and 52.8 HU in group 3. The average lung attenuation in the cranioventral aspect of the lung lobes (-140 ± 290.7 HU, range -828.0 to 64.3 HU) was higher than in the caudodorsal aspect of the lung lobes (-693.7 ± 121.0 HU, range -851.4 to 26.2 HU).

Disease group	Attenuation (HU) pre-contrast	Attenuation (HU) post-contrast	HU pre - HU post contrast difference
Group 1	-456.8 ± 81.9 [-898.9 - 76.6]	-424.1 ± 82.3 [-871.9 – 120.4]	32.7 ± 14.6 [11.9 – 54.3]
Group 2	-478.2 ± 123.2 [-851.5 – 123.2]	-451.1 ± 130.3 [-836.2 – 125.8]	24.5 ± 17.8 [-1.3 – 49.3]
Group 3	-521.9 ± 164.1 [-869.1 – 164.0]	-491.5 ± 165.0 [-841.2 – 108.1]	30.4 ± 11.2 [16.1 – 52.9]

Table 3-1 Summary of the average ± stdev [range] lung attenuation in Hounsfield units (HU) pre- and post-intravenous iodinated contrast medium administration and the difference in attenuation between the pre- and post-intravenous iodinated contrast medium administration images sorted by group.
Group 1- acute, Group 2- short term chronic, Group 3- long term chronic

3.3.4 Comparison of Thoracic Computed Radiography and Computed Tomography for Pulmonary Disease Diagnosis

Both evaluators detected abnormal lung patterns, consistent with pulmonary disease, in all 30 calves with CT. Using the CT diagnosis of the more experienced evaluator as gold standard, the more experienced evaluator (SSV) also detected abnormal lung patterns in all 30 calves with CR. This was repeated when only the cranioventral quadrant was assessed, in which all patients had disease identified on both CT and CR. Using CR, the less experienced evaluator (JF) correctly identified 27 of 30 calves with abnormal lung patterns, and the three misidentified calves were chronic disease groups (two short-term and one long-term). Differences in abnormal lung detection between imaging modalities were not statistically significant ($p=0.25$).

The severity of pulmonary disease diagnosis was evaluated based on lung pattern, for which alveolar was considered the most severe pulmonary disease pattern. The more experienced evaluator detected alveolar lung patterns in 29 calves using CT and correctly identified 28 of these calves as having an alveolar lung pattern and 1 calf as not ($n=1$)

using CR. The less experienced evaluator identified correctly 29 of 30 calves having either an alveolar lung pattern (n=28) or not (n=1) with CT and identified correctly 25 of these calves as having an alveolar lung pattern with CR. Four of the misdiagnosed calves were from the chronic diseases groups (two short-term and two long-term) and one calf was from the acute disease group. Differences in severity assessment between imaging modalities were not statistically significant (p=0.25).

Regardless of group, all of the calves had at least one lung quadrant with abnormal pulmonary patterns identified; none of the calves had a normal evaluation of all four quadrants of the lungs. In most calves (23 of 30 cases: group 1- 9 calves, group 2- 7 calves, group 3- 7 calves) all four quadrants had an abnormal lung pattern (Table 3-2). Four calves (group 1- 1 calf, group 2- 1 calf, group 3- 3 calves) had three abnormal lung quadrants. Three calves (group 2- 1 calf, group 3- 1 calf) had two abnormal lung quadrants. The craniodorsal and cranioventral quadrants had abnormal lung pattern in all calves. Of the two cranial quadrants, the ventral part was more severely affected, as alveolar lung patterns were observed only in the cranioventral but not in the craniodorsal quadrant in 8 out of 30 calves (p=0.01) by one evaluator (SSV) and 10 out of 30 calves (p=0.009) by the other evaluator (JF). The 3 calves with two abnormal lung quadrants had normal caudoventral and caudodorsal lung quadrants, whereas the 4 calves with three abnormal lung quadrants had normal caudodorsal lung quadrants.

total		**Ev1**	**0**	**0**	**30**	**0**	**0**	**30**	**0**	**2**	**28**	**0**	**7**	**23**	**120**
		Ev2	**0**	**3**	**27**	**3**	**2**	**25**	**0**	**6**	**24**	**0**	**4**	**26**	**120**
Cr-CrV	**Normal**	**Ev1**													**0**
		Ev2		1	2										**3**
	Bronchial	**Ev1**													**0**
		Ev2			1										**1**
	Interstitial	**Ev1**			1										**1**
		Ev2			1										**1**
	Alveolar	**Ev1**			29										**29**
		Ev2		2	23										**25**
CR-CrD	**Normal**	**Ev1**						1							**1**
		Ev2						4							**4**
	Interstitial	**Ev1**						8							**8**
		Ev2				2		4							**6**
	Alveolar	**Ev1**						21							**21**
		Ev2				1	2	17							**20**
CR-CrD	**Normal**	**Ev1**								2					**2**
		Ev2								4	2				**6**
	Interstitial	**Ev1**									8				**8**
		Ev2									7				**7**
	Alveolar	**Ev1**									20				**20**
		Ev2								2	15				**17**
CR-CdD	**Normal**	**Ev1**											7	3	**10**
		Ev2												1	**1**
	Interstitial	**Ev1**												9	**9**
		Ev2												5	**5**
	Alveolar	**Ev1**												11	**11**
		Ev2											1	20	**21**
Modality		**Evaluator**	**CT-CrV**			**CT-CrD**			**CT-CdV**			**CT-CdD**			**Total**
	Lung pattern		**Normal**	**Interstitial**	**Alveolar**	**Normal**	**Interstitial**	**Alveolar**	**Normal**	**Interstitial**	**Alveolar**	**Normal**	**Interstitial**	**Alveolar**	

Table 3-2. Summary of the lung pattern evaluation of each evaluator by modality (CR and CT) in each quadrant of the thorax. CR – computed radiology, CT – computed tomography, CrV – cranioventral, CrD – craniodorsal, CdV – caudoventral, CdD – caudodorsal

The less experienced evaluator (JF) was less likely to identify disease in the craniodorsal quadrant than the more experienced evaluator (SSV) (80 versus 100% (p=0.01). Similar trends were observed for the cranioventral quadrant (90% versus 100%) and the caudoventral quadrant (77% versus 90%). No clear trends were observed for the caudodorsal quadrant, as 5 calves were identified as abnormal only by SSV and 6 calves were identified as abnormal only by JF. No group differences were detected, when comparing the acute with the chronically diseased calves.

Both evaluators had a moderate to high agreement between CR and CT for identifying diseased lung and lung pattern in the cranioventral quadrant with a Kappa of 0.70 and 0.96, respectively. Similarly, the inter-observer agreement for CR showed a high correlation with 0.97 and a moderate for CT with 0.70 for the cranioventral lung aspects (Table 3-3). All other areas had a lower inter-observer correlation.

Quadrant	**CrV**		**CrD**		**CdV**		**CdD**		**Total**	
Evaluator	**Ev1**	**Ev2**	**Ev1**	**Ev2**	**Ev1**	**Ev2**	**Ev1**	**Ev2**	**Ev1**	**Ev2**
Agreement	29	23	21	17	20	15	11	10	81	75
by chance	1	7	9	13	10	15	19	20	39	45
Kappa	**0.97**	**0.70**	**0.57**	**0.24**	**0.50**	**0**	**-0.73**	**0.5**	**0.52**	**0.4**

Table 3-3 Intra-observer agreement between the radiography (CR) and computed tomography (CT) identifying a normal and abnormal lung patterns in the four quadrants of the thorax. CrV – cranioventral, CrD – craniodorsal, CdV – caudoventral, CdD – caudodorsal

The least agreement between the two modalities was noted in the dorsal and caudal aspects of the lung (Table 3-4). Both evaluators identified the cranioventral quadrant as the most severely and extensively affected quadrant in all three groups. Alveolar pattern was frequently detected in the cranioventral quadrant on both CT (97%) and CR (93%), and the cranioventral quadrant had the highest area of alveolar pattern

detected on both modalities (CT- 95%, CR- 93%).This was followed by the craniodorsal and caudoventral quadrants of the thorax. Of these two quadrants, the caudoventral was more extensively affected compared to the craniodorsal quadrant. The least affected quadrant in all groups was the caudodorsal quadrant in which 10% of calves had an alveolar pattern, and this was similarly reported by both evaluators.

Modality/ Quadrant	**CR-CrV**	**CR-CrD**	**CR-CdV**	**CR-CdD**	**CT-CrV**	**CT-CrD**	**CT-CdV**	**CT-CdD**	**Total CR**	**Total CT**
Agreement	29	21	20	11	23	17	15	20	87	69
by chance	1	9	10	19	7	13	15	10	33	51
Kappa	**0.97**	**0.57**	**0.50**	**-0.73**	**0.70**	**0.24**	**0**	**0.50**	**0.62**	**0.26**

Table 3-4 Inter-observer agreement for radiography (CR) and computed tomography (CT) identifying a normal and abnormal lung patterns in the four quadrants of the thorax. CR – computed radiology, CT – computed tomography, CrV – cranioventral, CrD – craniodorsal, CdV – caudoventral, CdD – caudodorsal

Generally, no significant differences were seen in the extent of affected lung between the three groups. The caudal quadrants tended to have a larger area of lung involved with longer disease duration. Otherwise, no strong correlation was noted between the lung pattern and length of disease course, or extent of diseased lung and length of disease course. In the earlier phase of disease (group 1) both evaluators had a better agreement in diagnosing lung pattern and extent of diseased lung. The largest disagreement between the evaluators was noted in the craniodorsal, caudodorsal and caudoventral quadrants of the thorax in regards to lung pattern present. However, both evaluators were in close agreement that the lungs were extensively diseased.

No pleural fluid was noted in either imaging modality. A slightly higher number of cases with pleural thickening were noted using CT than CR (83% using CT, compared to 76% using CR). The degree of pleural thickening ranged from mild to moderate, and

decreased mildly with chronicity of disease in all calves. In none of the cases, a diffuse or focal contrast enhancement of the pleura was noted. No statistically significant difference was noted between the acute and chronic diseases calves and between the individual groups.

No strong correlation was identified between the CR and CT imaging findings and the respiratory scores.

3.3.5 Histopathology and Microbiology

Similar to the imaging findings, all calves were histopathologically diagnosed with suppurative pneumonia. Two calves (one each in group 1 and 2) were histopathologically additionally diagnosed with necrotizing pneumonia. The cranioventral aspects of the lungs were the most commonly and severely diseased areas of the lungs. The more dorsal lung aspects were either normal or had only mild changes suggestive of pneumonia. One calf in group 3 had mostly normal lung with only small areas of minimal consolidation (Fig 3-2). In 1 calf (group 1), histopathology and microbiology results of the lung tissue were unavailable.

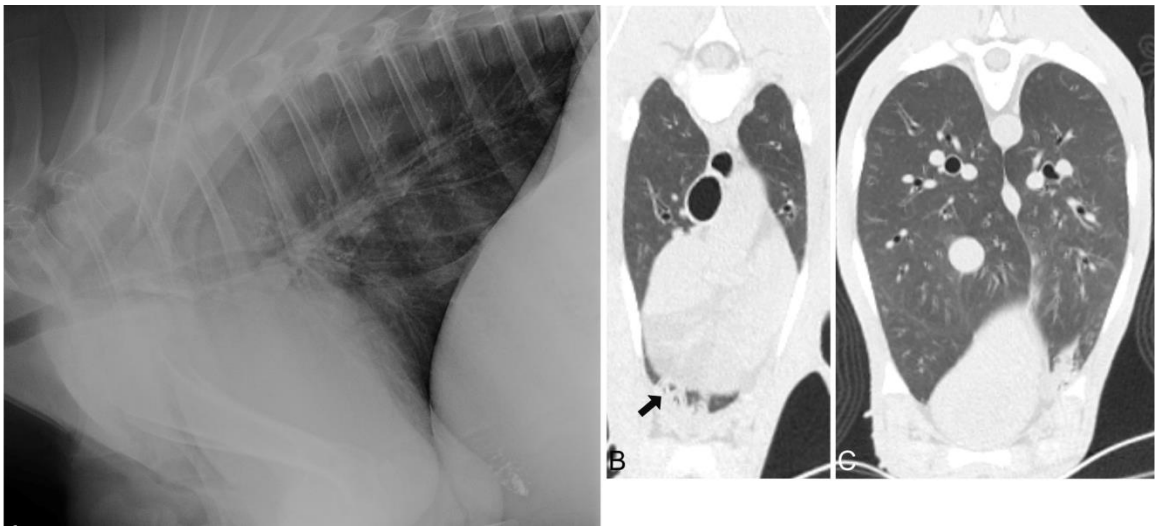

Figure 3-2 Radiographic and computed tomography images of the thorax of a calf from group 3 (chronic-long term respiratory disease) with a respiratory score of 7 and body temperature of 38.1C. No bacteria or *Mycoplasma bovis* were isolated. (A) Lateral radiograph of the thorax demonstrating minimal lung parenchymal changes of the most ventral and cranial aspects of the lungs. Most aspects of the lung are normally air filled. Transverse CT image of the cranial (B) and (C) caudal aspect of the lungs illustrating that only minimal alveolar changes are noted in the cranioventral aspects of the lungs and no pathology was noted caudoventral and –dorsal.

Twenty-three calves (group 1- 8 calves, group 2- 7 calves, group 3- 8 calves) had *Mycoplasma* isolated from the lung tissue (Table 3-5). *Mycoplasma bovis* was found in all but 3 positive cultures, in these 3 cultures *M. bovirhinis* was isolated. Additionally, in some calves other *Mycoplasma* species, including *M. bovigenitalium* (3 calves) and *M. alkalescens* (3 calves) were isolated. *Pasteurella spp*. was cultured from the lung tissue of 15 calves and all of these calves had co-infection with *Mycoplasma* (Fig. 3-3). Only one *Mycoplasma* positive calf in group 3 had no bacteria recovered from the lung tissue. Only two calves in group 3 were negative for *Mycoplasma* in the lung tissue and had infections with *Pasteurella multocida*. In only one calf in group 3, in which minimal changes were seen on histopathology, no *Mycoplasma* or bacteria were isolated from the lung tissue.

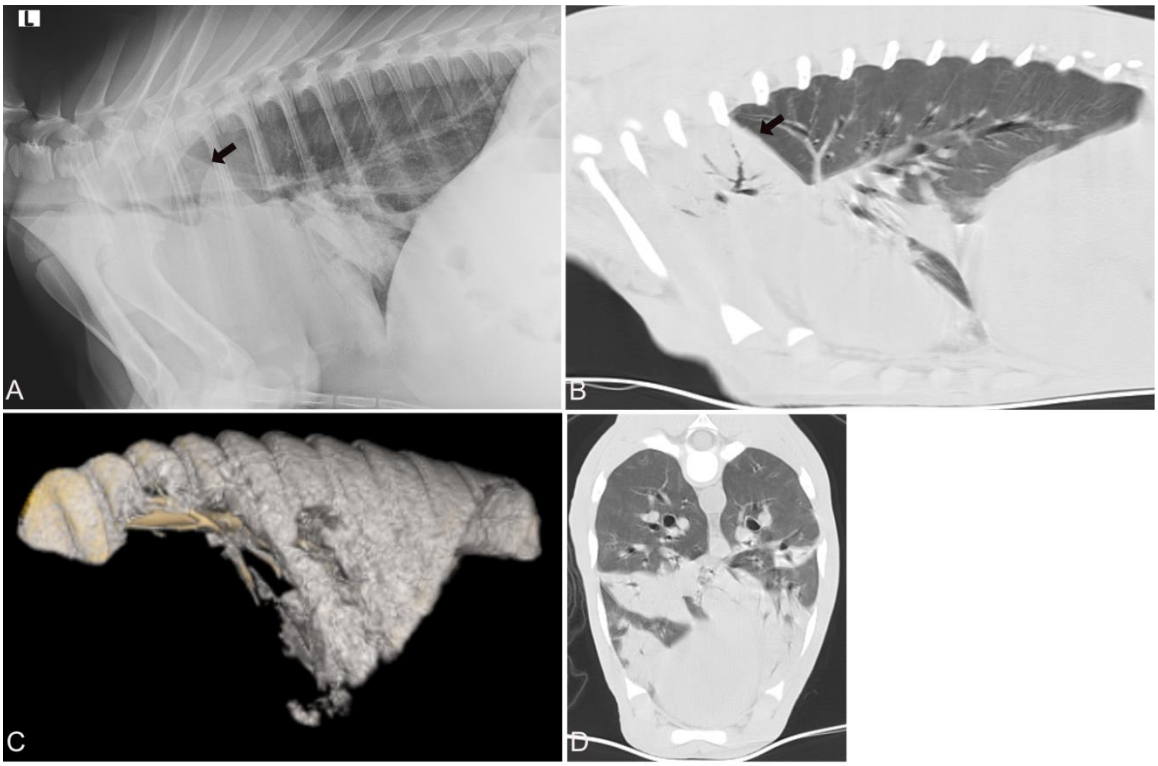

Figure 3-3 Radiographic and computed tomography images of the thorax of a calf from group 1 (acute respiratory disease) with a respiratory score of 7 and body temperature of 40.5C. *Mycoplasma bovis* was isolated and a bacterial coinfection was present. (A) Lateral radiograph and (B) sagittal reconstructed computed tomography (CT) image of the thorax in a lung window illustrating the alveolar lung pattern (*black arrow*) involving both cranial lung lobes, especially the right cranial lung lobe. (C) Three-dimensional (3D) reconstructed image of the air-filled lung. The cranial and cranioventral aspects of the lungs lack air-filling and are therefore not 3D reconstructed. (D) Transverse image of the thorax at the caudal aspect of the cardiac silhouette demonstrates the various regions in the lung with an alveolar lung pattern.

	Suppurative pneumonia	Necrotizing pneumonia	Mycoplasma in lung total	M. bovis in lung	Other Mycoplasma in lung	Pasteurella multocida	Mannheimia haemolytica	Other bacteria lung	Body temperature (C) Average ± stdev [range]	Respiratory score Average ± stdev [range]
Gr 1	10	1	8	6	M. bovirhinitis (1), M. bovigenitalium (4)	4	3	Mixed gram-positive bacteria (2), Arcanobacterium pyogenes (1)	40.1 ± 0.5 [39.5 – 40.9]	9.6 ± 1.5 [7 - 12]
Gr 2	10	1	7	6	M. bovirhinitis (1), M. bovigenitalium (1)	4	1	Mixed gram-positive bacteria (4), mixed gram-negative bacteria (2), Corynebacterium sp. (1)	39.3 ± 0.5 [38.5 – 39.9]	8.3 ± 1.6 [5 - 11]
Gr 3	10		8	7	M. Akalescens (2)	7	2	Mixed gram-positive bacteria (2), Bacillus sp. (1), Streptococcus sp. alpha-hemolytic (1)	38.7 ± 0.8 [37.6 – 39.5]	7.6 ± 1.8 [4 - 11]
Total	30	2	23	19	0	15	6			

Table 3-5. Summary table of the histopathology, mycoplasma speciation and bacteriology results including body temperature and respiratory scores sorted by groups Gr 1 – acute respiratory disease, Gr 2 - short-term chronic respiratory disease, Gr 3 - long-term chronic respiratory disease

3.4 Discussion

In our study radiographs of the calves were obtained in standing position, in all but one calf. All radiographs allowed evaluation of the cranioventral lung area and diagnosis of the area as diseased despite the summation with the forelimbs. In one study, calves were lifted from the floor to extend the front legs cranially,(17) which required at least three persons holding the patient and pulling the legs away from thorax. In our study, usually only one person was holding the standing calf, which minimized the number of people close to the radiographic beam. This also decreased handling of the

patient, which might further reduce the stress in the case of a respiratory distressed patient. Although intravenous sedation can be utilized to decrease the patient's stress and for chemical restraint, all calves enrolled in this study tolerated standing radiographs well while being awake. Furthermore, sedation may result in a decreased respiratory rate and effort and may therefore lead to incomplete aeration of the lung (atelectasis), which can be confused with lung disease such as pneumonia.

The intravenous sedation protocol utilized in this study provided a plane of sedation that was adequate for acquiring MDCT images of diagnostic quality without requiring repeat CT scanning. This is consistent with reports in small animals describing the use of MDCT in awake or sedated animal for the acquisition of pelvic CTs for trauma evaluation in dogs,(14) the abdomen in dogs with acute abdominal signs,(13) and studies of the cat respiratory tract for assessment of upper airway obstruction.(12) Although calves with respiratory disease commonly have tachypnea and cough as well as other signs of respiratory compromise, the plane of sedation provided by the sedation protocol described herein allowed acquisition of CT images with a generally mild degree of respiratory motion, which did not preclude evaluation of the bronchial tree or pulmonary vasculature or parenchyma. In this study, the intraluminal contents of the bronchi could be evaluated to the level of the tertiary bronchi with ease in almost all cases. Although a degree of blurring of the smaller airways was appreciated in most of the patients, an evaluation of the Hounsfield units could be made to enable identification of a lack of air-filling and abnormal intraluminal content.

The increased degree of respiratory motion noted in the post-contrast enhanced MDCT images is likely due to the longer time post administration of sedation, but could

in part also be due to the intravenous administration of a low-osmolar non-ionic iodinated contrast agent (iopamidol). It cannot be excluded that some of the calves had an immediate drug reaction leading to an increase in respiratory rate; however, currently no immediate adverse contrast agent reactions are reported in bovine species. For comparison, the percentage of immediate allergic drug reactions reported in human patients post injection of a non-ionic low-osmolar non-ionic iodinated contrast agent is low ranging between 0.2% to 2.7%. The human allergic drug response most frequently reported post intravenous low-osmolar non-ionic iodinated contrast agent injection included rash (85.3%), itching sensation (58.8%), nausea and vomiting (6.8%) followed by dyspnea, which was reported in 4.8% of cases in one study.(18) No rash was noted in any of the calves post contrast agent injection. However, several of the signs noted as an immediate drug reaction in human patients could not be assessed in these calves. No anaphylactic responses secondary to the iopamidol contrast agent injection were noted in any of the calves in this study. Intravenous contrast medium was administered in this study to assess if the contrast enhancement pattern or degree could be utilized as an indicator of lung disease and disease duration; however, no statistically significant differences were seen in the enhancement between the three groups. Contrast medium enhancement can be utilized to identify if soft tissue attenuating material within the pleural space is due to fluid or vitalized tissue. In this study, no pleural fluid was seen in any patient. Had pleural fluid been present, assessment of which pleural layer, parietal or visceral, could have been performed. The pleural thickening seen likely involved both pleural layers, but the visceral component was likely more extensive given that the primary disease was within the pulmonary parenchyma.

The cranioventral aspects of the lungs were the most commonly and severely affected lung areas in both imaging modalities and on histopathology, which is similar to previous reports.(5) The least affected quadrant was the caudodorsal quadrant, and on CR the caudodorsal quadrant had the lowest disease detection rate (60%) (Fig. 3-4). As well, there was a higher variability of assessment between the examiners in the caudodorsal quadrant suggesting that this region is more difficult to diagnose as abnormal, especially in the chronic disease cases. Examination of the caudodorsal quadrant alone may be insufficient for detection of diseased patients.

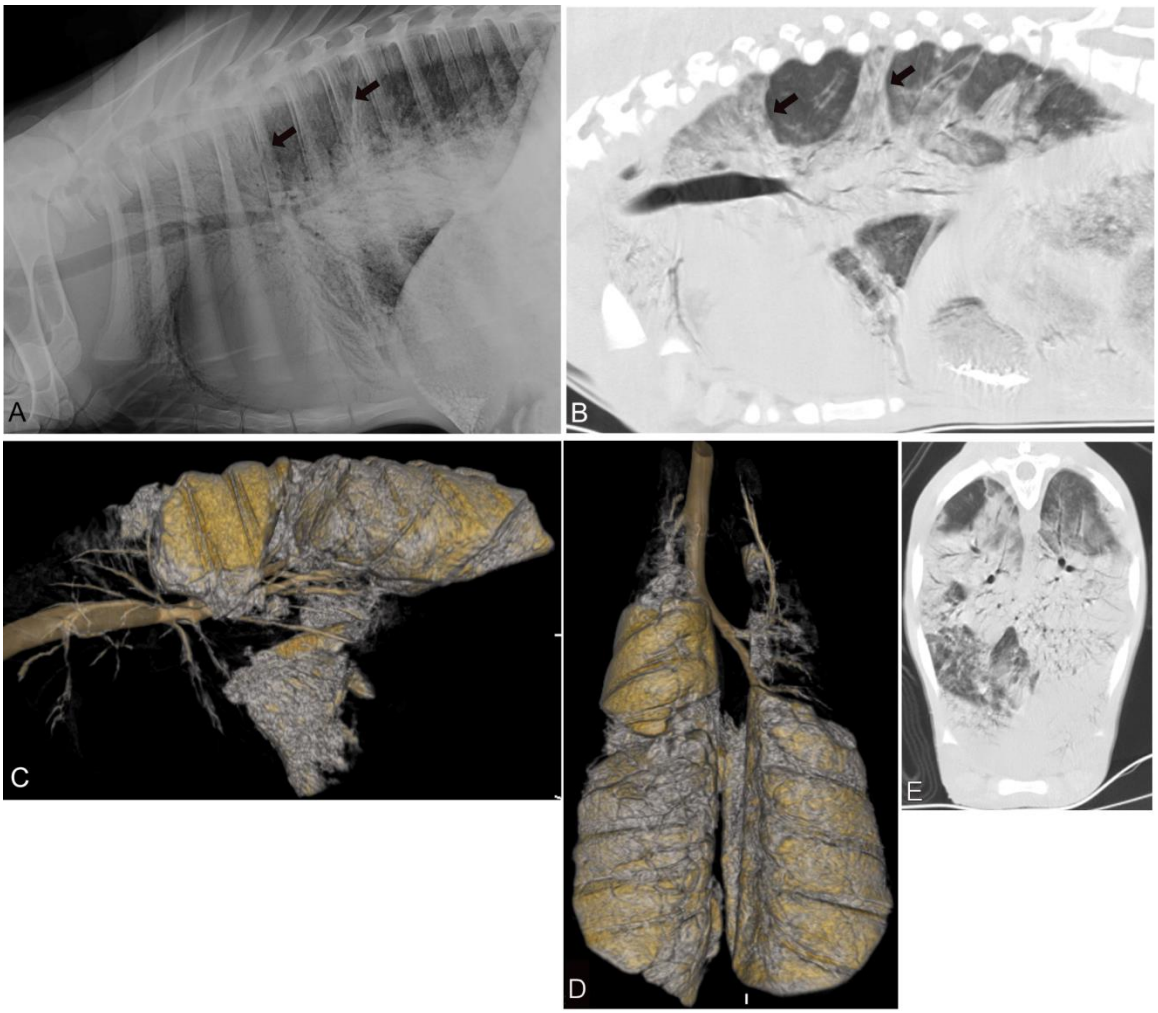

Figure 3-4 Radiographic and computed tomography images of the thorax of a calf from group 3 (chronic-long term respiratory disease) with respiratory score of 9 and body temperature of 39.1C. (A) Lateral radiograph and (B) sagittal reconstructed computed tomography (CT) image of the thorax in a lung window illustrating the various areas of alveolar lung pattern (*black arrow*) involving the cranial aspects of the thorax most severely and to a lesser extent the caudodorsal aspects of the lungs. Three-dimensional (3D) reconstructed sagittal (C) and dorsal (D) image of the air-filled lung. The entire cranial and in part caudoventral aspects of the lungs lack air-filling and are therefore not 3D reconstructed. (E) Transverse image of the caudal thorax illustrating the various areas with a severe lung pattern occupying nearly all aspects of the lung parenchyma.

It is important to consider that the caudodoral lung parenchyma may be more normal than the lung of the more cranial and ventral thorax when imaging studies are performed as it has been suggested that radiographs of the caudodorsal thorax are more

easily obtained likely due to the lack of summation with the soft tissues from the forelimbs, and requiring less high exposure values, when compared to the cranioventral thorax using radiography.(5) Given that radiography is a more accessible as an on-farm imaging modality for veterinarians, this is likely especially important to consider when attempting high quality thoracic radiographs using mobile radiographic units under field conditions where higher radiographic output setting to penetrate the cranioventral aspect of the thorax might not be available. Furthermore, obtaining radiographs of just the cranioventral aspect of the lungs might be sufficient to diagnose pneumonia as these areas were diagnosed with disease in more than 93% of the calves. However, none of the calves was diagnosed as completely normal by either of the evaluators using CR when the entire thorax was radiographed, which is consistent with the histopathology reports where all calves were diagnosed with pneumonia. Experience level impacted the assessment of severity of pulmonary disease, as the less experienced evaluator may underscore severity of disease based on imaging findings, this is unlikely to be clinically significant as the calves were still diagnosed with pulmonary disease requiring treatment. No significant difference between imaging modalities was found. Given these findings, CR and CT are likely equally effective in diagnosing acute and chronic pulmonary disease.

No strong correlation was seen between the clinical respiratory scores and the severity of disease on CR and CT. Mismatch between clinical severity and imaging severity is consistent with the concept of a lag between clinical disease and development of imaging abnormalities.

All calves were histopathologically diagnosed with suppurative pneumonia and

two calves had additionally a necrotizing pneumonia. Only one calf had minimal lung changes identified histopathologically. Furthermore, abnormal lung patterns identified on imaging correlated well with the histopathology disease diagnosis. This has similarly been suggested for radiography in a previous experimental study.(17)

The vast majority of the calves in the study had *Mycoplasma* isolated from lung tissues, and two thirds of those had a co-infection with *Pasturella spp*. This is similar to human studies, in which *Mycoplasma* is known to be a common agent for acute respiratory infection. Furthermore, it is known from human studies that *Mycoplasma* infection may precede and cause subsequent more severe infections with other viruses and bacteria due to immunosuppression and alteration of the normal respiratory flora by the *Mycoplasma* infections.(19,20) Only one *Mycoplasma* positive calf did not have a coinfection with other bacterial pathogens. It is possible that a fastidious organism was present, but was not isolated. Future work such as this should include diagnostics with commercially available viral and bacterial bovine respiratory disease PCR assays.

As all the calves in the current study were diagnosed with pneumonia, an accuracy assessment could not be obtained. This limits the study in that we were unable to extrapolate the utility of the tests for a herd assessment tool. If animals without infectious pneumonia have pulmonary changes on imaging that are similar to findings associated with pneumonia, a false positive test result could occur. False positive diagnoses would lead to unnecessary antibiotic therapy, which may increase the risk of development of antibiotic resistant bacteria and treatment costs. We had expected less severe lung parenchymal changes in the calves enrolled in this study and assumed that more lung areas would have a normal lung pattern therefore allowing to better compare

the imaging findings in normal and abnormal aspects of the lungs. However, it is important to note that imaging and histopathology findings were in agreement that the caudodorsal aspects of the lungs were the least affected or most normal aspects of the lungs suggesting that both imaging techniques will allow differentiating between normal and abnormal lung parenchyma.

A potential weakness of the study is the low number of evaluators in each group (n=1); which has likely the largest effect when evaluating the differences between the evaluators. However, the comparison between both imaging modalities is likely less affected, especially considering that only minimal differences were noted.

In conclusion, both CR and sedated MDCT were equally effective in diagnosing acute and chronic pulmonary disease. Our results indicate than a less experienced evaluator can detect abnormal lung patterns with CR and MDCT; however, a less experienced evaluator may underscore disease severity. Although acute and chronic pulmonary disease severity can be assessed by both evaluators with both modalities. Furthermore, thoracic MDCT can be safely be performed in sedated calves providing images of diagnostic quality. Combing clinical respiratory scores and imaging findings was inadequate for diagnosing chronicity of pneumonia in calves with naturally occurring pneumonia.

3.5 Footnotes

[a] FCR ClearView CS IIP and Type C IP, Fujifilm Co., Tokyo, Japan
[b] Toshiba Aquilion 64 CT, Toshiba America Medical Systems Inc., Tustin, CA
[c] Torbugesic®, Pfizer, New York, NY
[d] Ketaset®, Pfizer/Boehringer, St. Joseph, MO
[e] Anased®, Lloyd Laboratories, Shenandoah, IA
[f] Isovue 300, Bracco Diagnostics Inc., Princeton, NJ
[g] Empower CTA, Bracco Diagnostics Inc., Princeton, NJ

[h] Beuthanasia ®-D Special, Schering-Plough Animal Health Corp, Union, NJ
[i] eFilm, version 3.3.0, Merge Healthcare, Hartland, WI
[j] Vitrea workstation, software version 6.3.2, Vital Images Inc., Minnetonka, MN
[k] GraphPad Prism, version 6.04, GraphPad Software Inc., La Jolla, CA

3.6 References

1. USDA. Dairy 2007 - Heifer calf health and Management practices on U.S. Operations. USDAAPHISVS,CEAH Fort Collins, CO [Internet]. 2010;(January):168. Available from: http://www.aphis.usda.gov/animal_health/nahms/dairy/downloads/dairy07/Dairy07_ir_CalfHealth.pdf
2. Wittum TE, Woollen NE, Perino LJ, Littledike ET. Relationships among treatment for respiratory tract disease, pulmonary lesions evident at slaughter, and rate of weight gain in feedlot cattle. J Am Vet Med Assoc [Internet]. 1996;209(4):814–8. Available from: http://www.ncbi.nlm.nih.gov/pubmed/8756886
3. Adams EA, Buczinski S. Short communication: Ultrasonographic assessment of lung consolidation postweaning and survival to the first lactation in dairy heifers. J Dairy Sci. 2016;99(2):1465–70.
4. Verschooten, F., W. Oyaert and RD. Radiographic diagnosis of lung diseases in cattle. Vet Radiol Ultrasound. 1974;15(1):49–59.
5. Bargai, Uri; Pharr, John W.; Morgan JP. Bovine radiology. Iowa State University Press; 1989.
6. SG. N. The equine thorax. In: DE T, editor. Textbook of veterinary diagnostic radiology. 6th ed. St. Louis, MO: Elsevier; 2013. p. 632–49.
7. Rizzi EB, Schinina' V, Cristofaro M, Goletti D, Palmieri F, Bevilacqua N, et al. Detection of Pulmonary tuberculosis: comparing MR imaging with HRCT. BMC Infect Dis [Internet]. 2011;11:243. Available from: http://www.pubmedcentral.nih.gov/articlerender.fcgi?artid=3184086&tool=pmcentrez&rendertype=abstract
8. Prather AB, Berry CR, Thrall DE. Use of radiography in combination with computed tomography for the assessment of noncardiac thoracic disease in the dog and cat. Vet Radiol Ultrasound. 2005;46(2):114–21.
9. Lubbers B V., Apley MD, Coetzee JF, Mosier DA, Biller DS, Mason DE, et al. Use of computed tomography to evaluate pathologic changes in the lungs of calves with experimentally induced respiratory tract disease. Am J Vet Res. 2007;68(11):1259–64.
10. Henao-Guerrero N, Ricco C, Jones JC, Buechner-Maxwell V, Daniel GB. Comparison of four ventilatory protocols for computed tomography of the thorax in healthy cats. Am J Vet Res. 2012;73(5):646–53.
11. Oliveira CR, Mitchell MA, O'Brien RT. Thoracic computed tomography in feline patients without use of chemical restraint. Vet Radiol Ultrasound. 2011;52(4):368–76.
12. Stadler K, O'Brien R. Computed tomography of nonanesthetized cats with upper airway obstruction. Vet Radiol Ultrasound. 2013;54(3).

13. Shanaman MM, Hartman SK, O'Brien RT. Feasibility for using dual-phase contrast-enhanced multi-detector helical computed tomography to evaluate awake and sedated dogs with acute abdominal signs. Vet Radiol Ultrasound. 2012;53(6):605–12.
14. Lee K, Heng HG, Jeong J, Naughton JF, Rohleder JJ. Feasibility of computed tomography in awake dogs with traumatic pelvic fracture. Vet Radiol Ultrasound. 2012;53(4):412–6.
15. Lascola KM, O'Brien RT, Wilkins PA, Clark-Price SC, Hartman SK, Mitchell MA. Qualitative and quantitative interpretation of computed tomography of the lungs in healthy neonatal foals. Am J Vet Res. 2013;74(9):1239–46.
16. McGuirk SM. Disease Management of Dairy Calves and Heifers. Vet Clin North Am - Food Anim Pract. 2008;24(1):139–53.
17. Tegtmeier C, Arnbjerg J. Evaluation of radiology as a tool to diagnose pulmonic lesions in calves, for example prior to experimental infection studies. J Vet Med Ser B. 2000;
18. Kim SR, Lee JH, Park KH, Park HJ, Park JW. Varied incidence of immediate adverse reactions to low-osmolar non-ionic iodide radiocontrast media used in computed tomography. Clin Exp Allergy. 2017;47(1):106–12.
19. Kashyap S, Sarkar M. Mycoplasma pneumonia : Clinical features and management. Lung India [Internet]. 2010;27(2):75–85. Available from: http://www.lungindia.com/text.asp?2010/27/2/75/63611
20. Parrott GL, Kinjo T, Fujita J. A compendium for Mycoplasma pneumoniae. Front Microbiol. 2016;7(APR).

Chapter 4- Comparison of Thoracic Radiography, Ultrasonography, Computed Tomography, and Histopathology for the Detection of Pneumonia in Dairy Calves

4.1 Introduction

Pneumonia is a common inflammatory disease affecting the interstitium, alveoli and/or bronchi of the lungs. Pneumonia is part of the bovine respiratory disease (BRD) complex, which is the most common disease complex in both dairy and feedlot/back-grounding facilities.(1,2) In feedlot facilities, morbidity from respiratory disease has been estimated at up to 13% of calves in the peri-weaning age,(3) and some dairy farms have recorded up to 100% of calves having been treated with antibiotics for BRD.(4) Adequate treatment of pneumonia is based on early diagnosis; however, pneumonia is not always diagnosed on the farm or in the early stages of the disease. Due to the high incidence of BRD complex, and the associated welfare and financial costs of the disease complex, diagnostic tests which can be quickly and easily utilized on the farm for the diagnosis of BRD complex in large groups of cattle are necessary.

On the farm, respiratory disease scoring methods (5–7) are used to detect calves with respiratory disease, but these methods are known to have limitations detecting calves with pneumonia and are predominantly only effective in detecting calves with acute respiratory disease and fever.(8,9) Thoracic radiography is the most commonly used imaging modality for lung evaluation and is used in combination with the calf's history to diagnose pneumonia. Limitations of thoracic radiography are the summation of anatomic structures and the inability to penetrate in adult large animals the entire thorax. An important concern with radiography is radiation exposure to staff and veterinarians

acquiring images, especially when a large number of animals need to be examined. Computed tomography (CT) is considered the imaging reference standard for detection of pulmonary diseases because CT allows high resolution and summation-free imaging of the lungs.(10,11) Concerns are that CT is generally only available in hospital settings, involves exposure to ionizing radiation, and is relatively costly thereby limiting the application for diagnosis and monitoring of pulmonary disease in calves.

Currently only two studies describe the use of CT for assessing pulmonary disease in calves.(12,13): one in calves with experimentally induced pneumonia from *Mannheimia haemolytica* and the second in six calves during the first 105 days of life. Both studies lack comparison of the imaging findings with histopathology.

During the last decade, thoracic ultrasonography (US) has been increasingly utilized to diagnose and monitor various pulmonary diseases such as volume of pleural fluid,(14) pneumothorax,(15) pneumonia,(15,16), cardiogenic edema,(17) and traumatic rib fractures.(18) Compared with thoracic radiography and CT, thoracic US is cheaper, avoids radiation exposure, and can be implemented for on-farm diagnosis. A drawback of thoracic US is the lack of ultrasound beam penetration through normally air-filled lung inhibiting assessment of parenchymal lesions deep to the air-pleura interface.

Currently no study has been published in calves comparing the accuracy of thoracic CT, with thoracic digital radiography (DR) and pulmonary US for the detection of naturally occurring pneumonia. The purpose of this study was to assess the ability and accuracy of diagnosing pulmonary disease using thoracic DR, pulmonary US, and thoracic CT in comparison to histopathology and clinical disease scoring utilizing the Wisconsin method in calves with naturally acquired pulmonary disease. We hypothesized

that the diagnostic accuracy of US for identifying and localizing pneumonia is similar to thoracic DR and CT. Additionally, we hypothesized that thoracic imaging, regardless of modality, would be more sensitive than clinical respiratory scoring via the Wisconsin method for diagnosing pneumonia.

4.2 Materials and Methods

4.2.1 Animals

Sixteen pre-weaned Jersey heifer calves diagnosed by the on-farm veterinarian with persistent signs of respiratory disease despite two or more courses of antibiotic treatments were enrolled in the study (PNEUM group). Calves were suspected to have pulmonary disease due to clinical signs consistent with pneumonia including coughing, fever, dyspnea and nasal discharge. Additionally, six pre-weaned, clinically healthy Jersey bull calves with no history or current clinical signs of pulmonary disease were obtained from a different farm and included as control animals (HEALTH group).

All calves were transported to the Lois Bates Veterinary Teaching Hospital at Oregon State University for the imaging studies. Each group of calves were housed separately with free choice of water, grass hay, and pelleted creep feed, and were fed milk replacer twice daily until the imaging studies were performed. Calves were maintained in small groups in isolated hospitalization stalls, with hourly stall side monitoring by hospital staff, and twice daily complete physical examinations by a veterinarian (JF). All calves were allowed at least one night (12+ hours) to acclimate to the facility before imaging studies were performed. The study was approved by the Institutional Animal Care and Use committee at Oregon State University.

Immediately prior to imaging, physical examinations were performed and a clinical respiratory score was assigned to each calf based on the Wisconsin Calf Respiratory Scoring (RS) system.(19) Using this RS system, each of the following parameters was measured or evaluated in each calf: body temperature, the presence of a cough, nasal discharge, and ocular discharge or abnormal ear/head position. Each of these parameters was assigned a score of 0-3 based on severity, with 0 being normal and 3 being most severe. (20)

4.2.2 Image Acquisition

In each calf, the right and left thoracic walls were clipped and brushed clean immediately prior to imaging. All calves were first imaged using thoracic DR, followed by pulmonary ultrasound, and last thoracic CT.

4.2.2.1 Thoracic Digital Radiography

Standing left-to-right lateral thoracic digital radiographs (DR) were obtained with a wireless digital flat panel detector[a] at 90kVp and 32mAs. An attempt was made to include the entire thorax on a single projection, but a second lateral radiograph was obtained for larger calves to include the entire thorax.

4.2.2.2 Pulmonary Ultrasound

Isopropyl alcohol-70% was liberally applied to the right and left lateral thoracic wall to provide adequate coupling of the ultrasound probe. Ultrasound images were obtained with the transducer aligned with the intercostal space in transverse thoracic planes (parallel to the ribs) in the dorsal, mid, and ventral aspect of each intercostal space of the left and right hemithorax as well as each side of the thoracic inlet using a linear 5-

13MHz transducer[b]. All ultrasound images were labeled by location in which the image was obtained.

4.2.2.3. Thoracic Multi-Detector Computed Tomography

An intravenous catheter was placed aseptically into the left jugular vein immediately prior to the thoracic CT study. Each calf was administered a multimodal sedative protocol of 0.33 mg/kg ketamine,[c] 0.33 mg/kg xylazine,[d] and 0.11 mg/kg butorphanol[e] through the jugular vein catheter. Each calf was positioned in sternal recumbency on the 64-row multidetector CT scanner[f] table using the following imaging parameters: 0.5 mm collimation, 0.5mm reconstruction interval, 1 sec tube rotation time, 120 kVp, 400 mA, 0 tilt, and a pitch factor of 0.828. Each calf was imaged from cranial to the thoracic inlet to the mid-level of the left kidney to ensure that the entire thorax was included in the study. The thin collimated CT data were used to create transverse, dorsal, and sagittal reconstructed images of the thorax in 3 mm slice thickness. A bone, soft tissue, and lung algorithm was used to create bone, soft tissue, and lung window images. All imaging studies were sent to a dedicated PACS server for storage and later image analysis.

4.2.3 Necropsy and Histopathology

After image acquisition was completed, the calves were humanely euthanized with pentobarbital 960 mg/mL[i] at a dosage of 1mL/4.5 kg and submitted for necropsy. This included examination for concurrent non-respiratory disease in addition to assessment of the respiratory tract and tympanic bullae. Fifteen lung samples of approximately 2 cm^3 were obtained from each calf for histopathologic examination. Five for of these were obtained from the following samples sites in each calf: the caudal part

of the right cranial lung lobe ventral to the trachea, the ventral aspect of the right caudal lung lobe, the central aspect of the accessory lung lobe, the mid to lateral aspect of the cranial part of the left cranial lung lobe, and the most caudodorsal aspect of the left caudal lung lobe. Ten additional lung samples were collected from various locations in each calf: five based on imaging findings by one image evaluator (JF) and five based on gross necropsy findings by the pathologist (RB). If gross pathologies were noted in the lung area, sampling was performed at the interface of visually healthy and diseased lung. The goal for these lung samples was to evaluate whether gross necropsy and imaging findings would correspond. Each sample site was mapped on an outline of the bovine lung for each calf to ensure that each sample was taken at the correct spot and also to allow for later comparative image assessment (Fig 4-1). The mapping allowed uniform site evaluation among examiners and to compare histopathology and image findings.

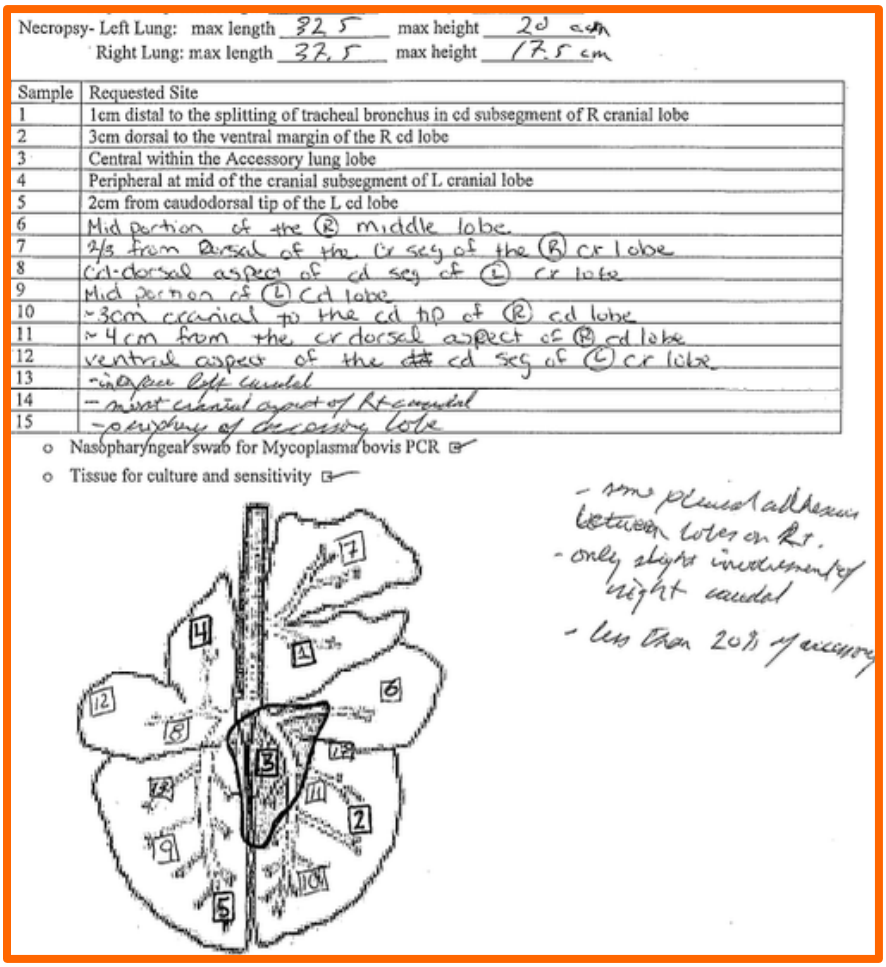

Figure 4-1 An example of a completed sample site map used for comparative image evaluation. Sites1-5 were the same sample sites in all calves. The remaining ten sites were selected for each calf separately: sites 6-10 were selected by one of the imaging evaluators (JF), sites 11-15 were selected by the pathologist (RB).

Samples were collected into 10% neutral-buffered formalin for routine processing and staining with hematoxylin and eosin (HE). These HE slides were assessed for changes in tissue architecture and for the degree of cellular infiltration of air spaces and interstitium (RB). These changes were classified utilizing a scoring system devised with the intent to delineate normal from abnormal lung tissue, assess the severity of changes and to separate changes primarily affecting the interstitial or alveolar space similar to the scoring system for the diagnostic imaging studies. For histopathology, a score of 1

denoted normal pulmonary parenchyma with or without evidence of atelectasis. A score of 2 was utilized to identify pulmonary tissue in which mild to moderate changes were seen affecting either predominately the bronchial or interstitial lung tissue. A scored 2 included changes such as bronchitis, bronchiolitis, alveolar/interlobular septal thickening. A score of 3 denoted abnormal lung tissues that included pathologies in the alveolar space, such as lung tissue consolidation, and lung tissue necrosis.

Furthermore, the thorax was evaluated for the presence or absence of pleural fluid, and air-filled thin- or thick-walled cavitary structures (e.g. bullae, pleural blebs, or abscesses), which were dichotomously recorded as present or absent.

Bacteriologic evaluation was performed at the Oregon State Veterinary Diagnostic Laboratory (Corvallis, OR) as follows: each calf was tested for *Mycoplasma bovis* polymerase chain reaction (PCR) using a nasopharyngeal swab sample. Additionally, bacterial culture was performed on lung tissue samples from the calves with clinical respiratory disease, and from nasopharyngeal swabs on the clinically healthy calves.

4.2.4 Image Evaluation

All diagnostic imaging studies were evaluated independently by two evaluators (JF, SS) using a commercially available DICOM viewer software[j]. All images of each modality and each calf were evaluated at the same location, which was estimated to be at approximately the location the lung tissue sample was obtained (Figure 4-1). This was done by assigning a three-piece location descriptor to each sample site as directed by the maps provided during histopathology sample collection. The three-piece descriptor included: left or right thorax; intercostal space estimated from the location of the tracheal

bifurcation on thoracic DR or CT images in relation to the region of lung sampled; dorsal to, at the level of, or ventral to the trachea. A list of these descriptors was provided to each image evaluator to enable uniform image assessment among evaluators and comparison of imaging and histopathology results.

Only standing left-to-right lateral projections were obtained for DR. Thus, any sample sites that were located at the same intercostal space and level (ventral, mid, dorsal) but from the opposite hemithorax received the same score (e.g. a sample from the right fourth intercostal space dorsally and the left fourth intercostal space dorsally would receive a score of 1 for both sample locations if that region was normal on radiographs).

For DR, the accessory lung lobes in standing calves cannot be distinctly identified as separate from the other lung lobes due to summation with the ventral aspects of the caudal lung lobes; however, the region of the accessory lung lobe was scored in DR as part of the summating structures in the caudoventral thorax between the cardiac silhouette and diaphragm. The accessory lug lobe is in standing calves using ultrasound not accessible from the thoracic wall and therefore no US images of the accessory lung lobe were obtained.

A 3-point scoring systems based on imaging pattern was used for all imaging modalities: a score of 1 denoted healthy, normal lung tissue as evidenced by well-defined pulmonary vascular and bronchial margins in DR and CT images (Fig 4-2) and only A-lines being present in US images (Fig 4-2). A-lines are hyperechoic lines coursing in parallel to the pleural surface, occurring secondary to a reverberation artifact at the pleura to air-filled lung interface (Fig 4-2).

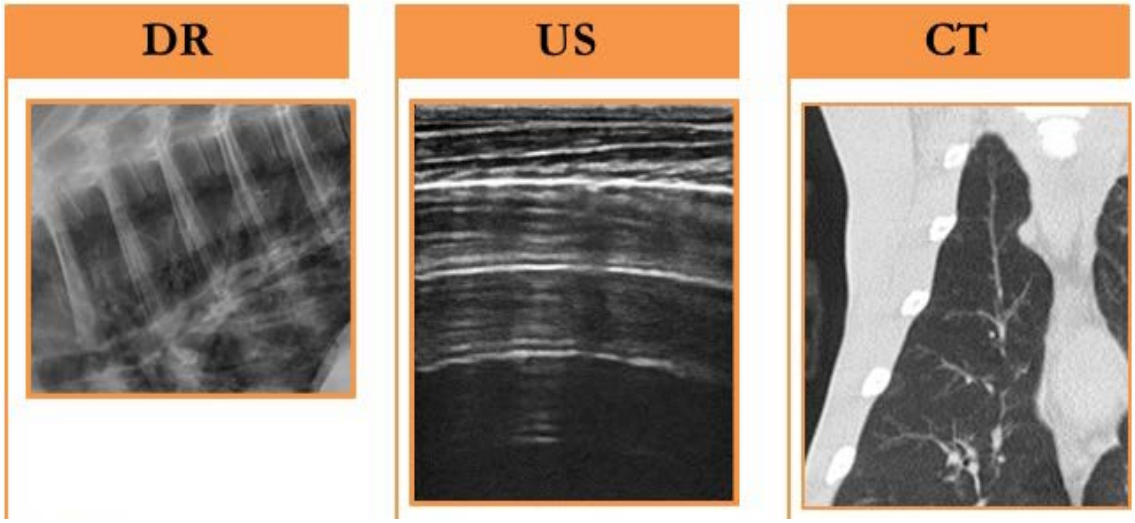

Fig 4-2: Normal pulmonary parenchyma, imaging score 1. DR- lateral projection of the caudodorsal thorax in which the pulmonary parenchyma is normal in opacity with the pulmonary vascular margins being well-defined. US- transverse plane image of the lung with normal A-lines due to a well-defined pleural interface with adjacent air-filled lung causing evenly spaced reverberation artifacts. CT- Dorsal plane lung window exhibiting normal pulmonary parenchyma with well-defined pulmonary vascular markings extending to the periphery of the lung lobes.
DR- Digital radiography, US- Ultrasound, CT- Computed tomography

A DR or CT score of 2 denoted bronchial and/or interstitial pulmonary patterns, as evidenced by bronchial wall thickening or an increased attenuation of the lung parenchyma resulting in a reduced definition of the pulmonary vasculature or bronchial margins (Fig 4-3). An US score of 2 was assigned when B-lines (lung rockets, comet tails) were present. B-lines were hyperechoic lines in perpendicular orientation from the pleural surface to the far field in the lung with nearly no reduction in echogenicity. These B-lines could either be single or multiple lines, and if multiple B-lines were present, they could also be confluent to one broad B-line (white lung).

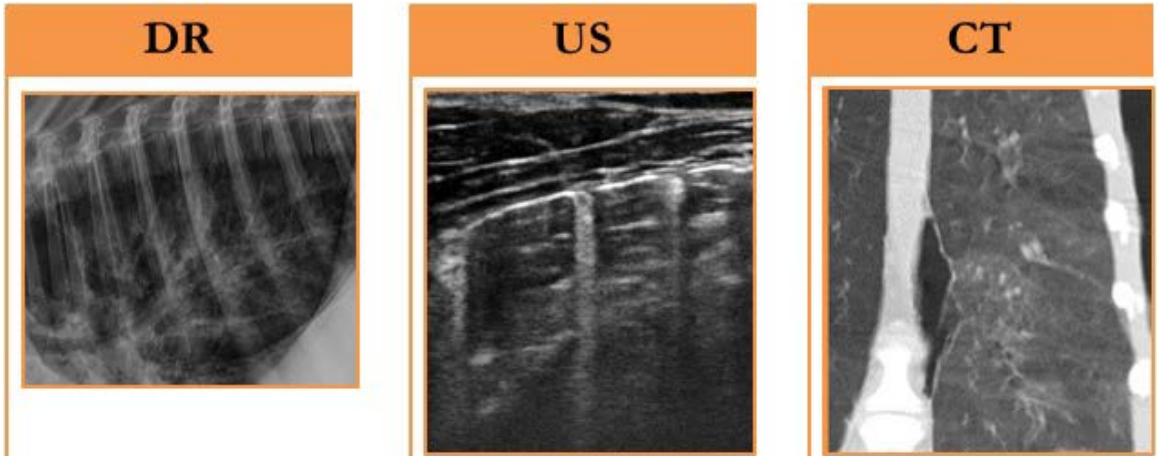

Fig 4-3: Imaging score 2. DR- Lateral projection of the caudodorsal thorax with a moderate unstructured interstitial pattern causing multifocal loss of distinction of the pulmonary vascular margins. US- transverse plane image of the thorax with at least three B-lines causing disruption of the normal pleural interface. CT- Dorsal plane CT image in lung windowing with multiple angular regions of increased attenuation of the pulmonary parenchyma causing loss of definition of the pulmonary vascular margins. DR- Digital radiograph, US- Ultrasound, CT- Computed tomography

The lung changes were scored as 3 on DR and CT if an alveolar pattern was noted. Alveolar patterns were defined by soft tissue attenuation of the pulmonary parenchyma, presence of one or more air bronchograms within the abnormally attenuating lung, and/or lobar signs at the interfaces of lung lobes with different severities of parenchymal disease (Fig 4-4). In US, a score of 3 was denoted for presence of "hepatized" lung tissue ("shred" or "tissue" sign), which was due to severe disruption of the pleural interface, and regions in which the degree of loss of air filling and cellular infiltration caused the lung to have an echotexture similar to that expected from non-lung tissue such as the liver (Fig 4-4).

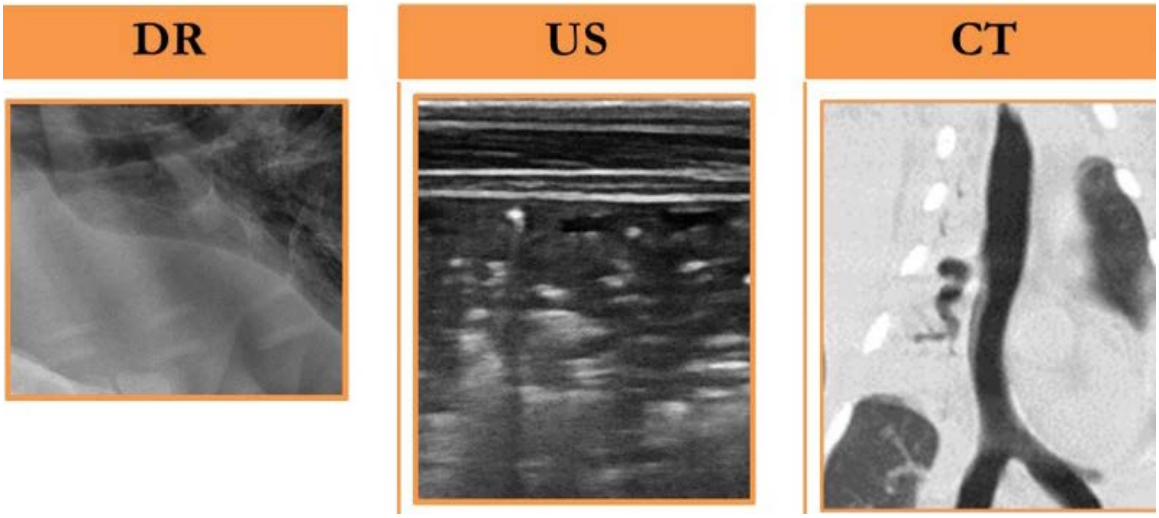

Fig 4-4: Imaging score 3. DR- Lateral radiograph of the cranioventral thorax showing an alveolar pattern with a lobar sign summating with the cardiac silhouette ventral to the trachea. US- transverse plane image showing complete loss of the normal A-line due to "hepatization" of the lung. CT- Dorsal plane CT image in a lung window with an alveolar lung pattern in the right cranial lung lobe and causing a lobar sign between the right cranial and middle lung lobes.
DR- Digital DR, US- Ultrasound, CT- Computed tomography

In addition, all imaging studies were evaluated for the presence or absence of pleural fluid, pleural gas and pulmonary parenchymal cavitary structures.

4.2.5 Statistical Assessment

Statistical analysis was performed with commercial software.[l,m] Quantitative data were assessed for normality using the Kolmogorov-Smirnov normality test and reported as mean ± standard deviation. For comparisons between disease groups, quantitative, normal distributed data were analyzed using a one-way ANOVA with Sidak's multiple comparisons tested adjustment for group differences; not normal-distributed quantitative data were analyzed using Wilcoxon rank sum test, and binary data were analyzed using Fisher's exact test.

For comparisons of imaging modalities within calf, comparisons of lung lobes within the same calf, and for comparison of evaluators within the same calf, multinomial categorical data were analyzed using a Wilcoxon matched pairs singed rank test and paired data were analyzed using McNemar's test. Categorical data with more than two categories (i.e., disease severity) were collapsed to binary data (i.e., healthy vs. diseased), if one category dominated the other categories. Inter- and intra-observer agreements were calculated for multinomial categorical data and statistically analyzed using kappa statistics. Statistical significance was set at $p < 0.05$.

4.3 Results

4.3.1 Animals

The sixteen pre-weaned Jersey heifer calves with clinical signs of pneumonia (PNEUM group) ranged in age from 56 to 109 days (mean: 77.7 ± 16.0 days; median: 64.5 days). The healthy control group included six approximately 60-day old clinically healthy Jersey bull calves (HEALTH group).

4.3.2 Calf Respiratory Scores Using the Wisconsin Method

Calf RSs ranged between 1 and 2 in the HEALTH group (mean: 1.3 ± 0.5) and between 3 and 10 in the PNEUM group (mean: 6.9 ± 1.7). In the PNEUM group, all calves had variable degrees of coughing, all but one calf (93.7%) had a RS of at least 5, which is considered abnormal; 13/16 (81%) calves had nasal discharge and of these 5 also had ocular discharge; and 8/16 (50%) calves had an elevated body temperature with the highest being 40.2° C. In the HEALTH group, all calves had a normal body

temperature (reference range: 38.6-39.4° C), no discharge from the eyes, nose or ears, and no cough.

In the HEALTH group, none tested positive for *M. bovis*, two calves tested positive on nasopharyngeal swab culture for *Arcanobacterium (Trueperella) pyogenes*. Otherwise, all calves in the HEALTH group had only environmental bacterial species cultured from the nasopharyngeal swabs. In the PNEUM group, 11 (69%) calves tested positive for *M. bovis*. All calves of the PNEUM group tested positive on lung bacterial culture for either *P. multocida* alone (10/16), a combination of *P. multocida* and *M. haemolytica* (5/16), or a combination of *M. haemolytica* and *H. somni*(1/16).

4.3.3 Histopathology

All 22 calves had histopathologically identified pulmonary changes consistent with pneumonia; in the HEALTH and PNEUM groups, 80 and 92% of sample sites, respectively, were scored as abnormal or diseased (Table 4-1). In the HEALTH group, 60% of the diseased sample sites were scored as an interstitial or bronchial pathology and 20% as having alveolar pathology. In contrast, the proportion of interstitial and alveolar diseased sample sites were nearly equal in the PNEUM group. Necrosis of the lung tissue was only seen in samples from the PNEUM group.

Score	Group	Histopathology Number of sample sites (% of samples)
1	HEALTH	18 (20%)
	PNEUM	20 (8%)
2	HEALTH	54 (60%)
	PNEUM	115 (48%)
3	HEALTH	18 (20%)
	PNEUM	105 (44%)

Table 4-1: Absolute number of histopathologic scores of the samples sites and percentage of samples sites arranged by group. Histopathology: Score 1- normal, Score 2- bronchial or interstitial pathology, Score 3- alveolar pathology
HEALTH- healthy control calves, PNEUM- respiratory disease calves

The left cranial lung lobe is the only lung lobe in which histopathology scores differed between HEALTH and PNEUM calves ($p = 0.007$). A trend ($p = 0.06$) was observed for the left caudal lung lobe.

4.3.4 Imaging Procedures

All calves were imaged with each of the three modalities. Most calves required two radiographic views to image the complete lung. In DR images, the accessory lung lobe could not be delineated from ventral aspects of the caudal lung lobes.

One evaluator obtained US images in standing calves and did not require assistance. The lung parenchyma could be seen cranially on the left and right side of the thorax to the level of the 3rd to 5th intercostal space and the caudal aspects of the lungs extended to the level of the 8th-11th intercostal space on the left and to the 9th to 11th intercostal space on the right. Besides the accessory lung lobes, the dorsal aspects of the cranial lung lobes could not be imaged with US because the front limbs interfered and the transducer could not be placed between front limbs and thoracic wall; thus, fewer US images were available for scoring compared with DR and CT (185 US images scored by

the more experienced evaluator, 212 US images scored by the less experienced evaluator, and 330 images scored both with DR and CT by both evaluators).

Thoracic CT images were obtained from all sedated calves. Variable degrees of respiratory motion were observed and resulted in mild to moderate slice misregistration as evidenced by stair-step artifacts of bronchi and areas of mildly increased attenuation of lung parenchyma.

4.3.5 Imaging Findings Based on Clinical Status (HEALTH vs PNEUM Group)

In all imaging modality, all clinically healthy calves (Fig 4-5) had a small area of alveolar lung pattern on CT or DR or a “shred” sign on US in the ventral aspect of the right cranial lung lobe (Table 4-2). The percentage of samples with a score of 3 in the right cranial lung lobe ranged in the HEALTH group from 4-35%, which was lower than in the PNEUM group, where it ranged from 46-72%. Similarly, histopathology scored a 3 in 35% of the HEALTH group samples and 72% of the PNEUM group samples.

Lung Lobe	Modality	Evaluator	HEALTH Group			PNEUM Group		
			Number of samples (% of samples available)			Number of samples (% of samples available)		
			Score 1	Score 2	Score 3	Score 1	Score 2	Score 3
Right cranial	DR	1	12 (52%)	10 (43%)	1 (4%)	11 (22%)	6 (12%)	33 (66%)
	DR	2	4 (17%)	15 (65%)	4 (17%)	7 (14%)	13 (26%)	30 (60%)
	US	1	0	1 (100%)	0	2 (23%)	4 (31%)	6 (46%)
	US	2	2 (29%)	5 (71%)	0	2 (12%)	6 (35%)	9 (53%)
	CT	1	20 (87%)	1 (4%)	2 (9%)	16 (32%)	2 (4%)	32 (64%)
	CT	2	10 (43%)	9 (35%)	8 (35%)	9 (18%)	4 (8%)	37 (74%)
	Histo		5 (22%)	10 (43%)	8 (35%)	2 (4%)	12 (24%)	36 (72%)
Right middle	DR	1	1 (13%)	7 (88%)	0	3 (15%)	3 (15%)	14 (70%)
	DR	2	1 (13%)	6 (75%)	1 (13%)	3 (15%)	5 (25%)	12 (60%)
	US	1	3 (60%)	2 (40%)	0	5 (31%)	4 (25%)	7 (44%)
	US	2	0	7 (100%)	0	1 (6%)	5 (31%)	10 (63%)
	CT	1	6 (75%)	2 (25%)	0	4 (20%)	3 (15%)	13 (65%)
	CT	2	4 (50%)	4 (50%)	0	2 (10%)	4 (20%)	14 (70%)
	Histo		0	7 (88%)	1 (13%)	0	9 (45%)	11 (55%)
Right caudal	DR	1	14 (93%)	1 (7%)	0	25 (48%)	16 (31%)	11 (21%)
	DR	2	10 (67%)	5 (33%)	0	16 (31%)	25 (48%)	11 (21%)
	US	1	8 (53%)	7 (47%)	0	30 (58%)	17 (33%)	5 (10%)
	US	2	1 (14%)	6 (86%)	0	9 (26%)	16 (46%)	10 (29%)
	CT	1	14 (93%)	1 (7%)	0	15 (25%)	22 (42%)	15 (29%)
	CT	2	9 (60%)	6 (40%)	0	16 (31%)	22 (42%)	14 (27%)
	Histo		5 (33%)	9 (60%)	1 (7%)	7 (13%)	31 (60%)	14 (27%)

Table 4-2: Absolute number of scores of the samples sites in each lung lobe and percentage of samples sites in each lung lobe and modality separated by evaluator and modalities in each group. Evaluator 1- less experienced evaluator, Evaluator 2-more experienced evaluator, Score 1- normal, Score 2- bronchial or interstitial pathology, Score 3- alveolar pathology

Lung Lobe	Modality	Evaluator	HEALTH Group			PNEUM Group		
			Number of samples (% of samples available)			Number of samples (% of samples available)		
			Score 1	Score 2	Score 3	Score 1	Score 2	Score 3
Accessory	DR	1	3 (50%)	3 (50%)	0	3 (17%)	7 (39%)	8 (44%)
	DR	2	3 (50%)	2 (33%)	1 (17%)	0	9 (50%)	9 (50%)
	CT	1	5 (83%)	1 (17%)	0	6 (33%)	4 (22%)	8 (44%)
	CT	2	5 (83%)	1 (17%)	0	3 (17%)	4 (22%)	11 (61%)
	Histo		0	4 (67%)	2 (33%)	2 (11%)	6 (33%)	10 (56%)
Left cranial	DR	1	9 (50%)	9 (50%)	0	18 (45%)	7 (18%)	15 (38%)
	DR	2	7 (39%)	10 (56%)	1 (6%)	7 (18%)	20 (50%)	13 (33%)
	US	1	7 (78%)	2 (22%)	0	11 (52%)	5 (24%)	5 (24%)
	US	2	1 (11%)	7 (78%)	1 (11%)	3 (14%)	8 (38%)	10 (48%)
	CT	1	14 (78%)	4 (22%)	0	21 (53%)	4 (10%)	15 (38%)
	CT	2	9 (50%)	9 (50%)	0	9 (23%)	16 (40%)	15 (38%)
	Histo		4 (22%)	10 (56%)	4 (22%)	2 (5%)	16 (40%)	22 (55%)
Left caudal	DR	1	12 (60%)	8 (40%)	0	29 (48%)	18 (30%)	13 (22%)
	DR	2	11 (55%)	9 (45%)	0	22 (37%)	23 (38%)	15 (25%)
	US	1	11 (55%)	9 (45%)	0	22 (37%)	29 (49%)	8 (14%)
	US	2	2 (15%)	10 (77%)	1 (8%)	8 (15%)	30 (58%)	14 (27%)
	CT	1	14 (17%)	6 (30%)	0	21 (35%)	20 (33%)	19 (32%)
	CT	2	1 (5%)	13 (65%)	1 (5%)	7 (12%)	32 (53%)	21 (35%)
	Histo		4 (20%)	14 (70%)	2 (10%)	7 (12%)	41 (68%)	12 (20%)

Table 4-2 (continued): Absolute number of scores of the samples sites in each lung lobe and percentage of samples sites in each lung lobe and modality separated by evaluator and modalities in each group. Evaluator 1- less experienced evaluator, Evaluator 2-more experienced evaluator, Score 1- normal, Score 2- bronchial or interstitial pathology, Score 3- alveolar pathology

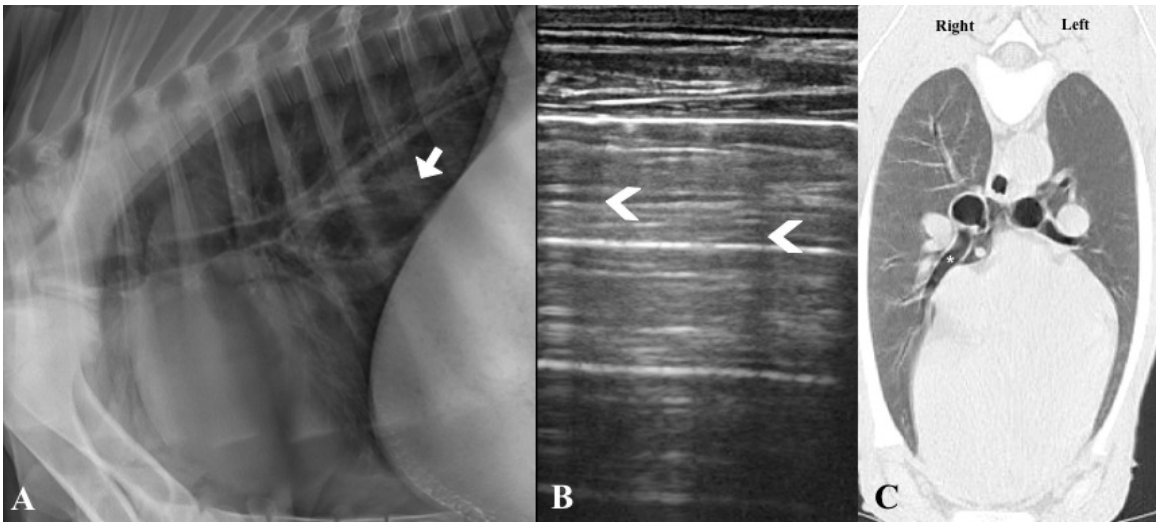

Fig 4-5: Thoracic DR, US and CT images of a clinically healthy calf with a normal respiratory score. On lateral DR (A), the pulmonary vascular margins are well-defined in most regions. A focal patch of unstructured interstital change is seen in the dorsal aspect of the caudal lungs (white arrow). An US image (B) acquired at the ventral aspect of the left 5th intercostal space shows a normal pleura to lung interface with evenly spaced A-lines. Thin hypoechoic lines are seen (white chevron) extending from the skin surface through the lungs consistent with contact artifact. On a lung window transverse plane CT image (C) immediately caudal to the tracheal bifurcation at the bronchus of the right middle lung lobe (asterix), the attenuation of the pulmonary parenchyma is normal.

The imaging difference between the HEALTH and PNEUM group was more noticeable in the left cranial lung lobe. Only 2 sample were scored a 3 by both evaluators and all imaging modalities together (6-11%) in the HEALTH group, whereas more than twice of the samples (24-48%) were scored a 3 in the PNEUM group. Similarly, more than twice of the samples in the PNEUM (44%) versus the HEALTH group (20%) were scored a 3 on histopathology (Table 4-1).

In the HEALTH group, US had the fewest sites scored of 3 regardless of evaluator (no sites in any lung lobe identified by evaluator 1, and 1 site in each the left cranial and left caudal lung lobes identified by evaluator 2); this is different from the

PNEUM group, which scored a 3 in all lung lobes (ranging from 10-63% of the samples sites in each lobe).

In all imagining modalities, clinically diseased calves had large areas of imaging patterns consistent with alveolar pathology in both cranial lung lobes (Fig 4-6). In 15/16 clinically diseased calves, extensive areas of imaging patterns consistent with alveolar pathology were present in the ventral aspects of all lung lobes. The remaining calf (RS of 6) had more focal small patches of alveolar lung pattern in addition to a few nodular, soft tissue attenuating structures. Both evaluators scored most of the imaging sites as either interstitial or alveolar pathology, which is in line with the histopathological findings. The more experienced evaluator was more in line with the clinical diagnosis of pneumonia. The smallest differences in lung imaging scores between evaluators were observed for DR.

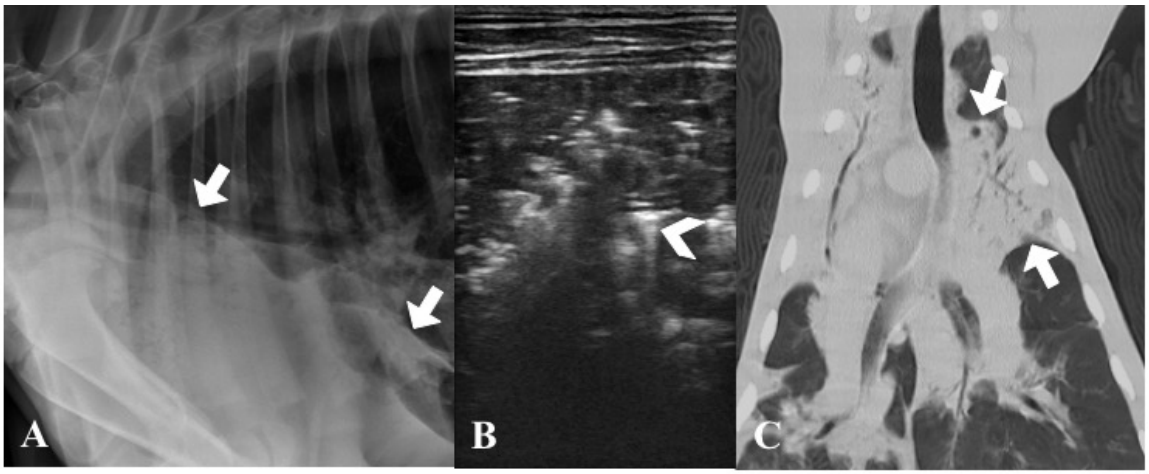

Fig 4-6: Thoracic DR, US and CT images of a calf with respiratory disease. On a lateral DR (A) projection and dorsal plane lung window CT (C) image, a severe alveolar pattern is present in the cranial lung lobes with lobar signs between the soft tissue attenuating lung and the more air-filled lung caudal to it (white arrows). These alveolar patterns correspond to regions of hepatization on US (B) in which the tissue has a loss of the A-lines from the lung-pleura interface allowing the penetration of the US waves deep into the diseased lung parenchyma. Several hyperechoic triangular shaped “comet tail” artifacts are present within the parenchyma consistent with trapped gas (white chevron).

Differences in CT and DR imaging scores between clinically healthy and diseased calves were obtained for the right caudal lung lobe and the accessory lung lobe (Fig 4-7). The limited number of US images precluded us to do meaningful statistics.

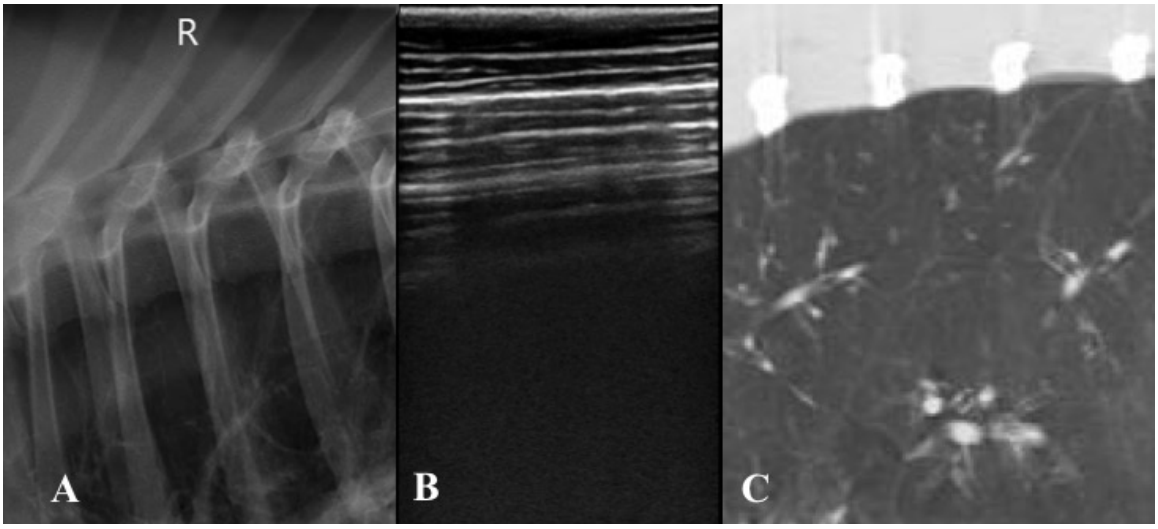

Fig 4-7: Thoracic DR, US and CT images at the dorsal aspect of the 8th intercostal space in a calf with known respiratory disease. This calf had a respiratory score of 7 due to a persistent cough, bilateral ear droop, and mild nasal discharge, but a normal body temperature of 38.1º C. On DR and CT (A), the pulmonary vascular margins are well-defined in the dorsal aspect of the 8th intercostal space corresponding to normal A-lines on US images (B).

4.3.6. Comparison of the Test Performance of the Imaging Modalities

4.3.6.1 Test Performance of the Imaging Modalities Compared to Histopathology

Imaging scores were categorized as either normal (score 1) or abnormal lung pathology (score 2 & 3). Using histopathology as reference standard, the diagnostic test performance of all three imaging modalities was similar within each individual imaging evaluator but differed between imaging evaluators. The less experienced evaluator underscored disease to a larger degree than the experienced evaluator but was better in scoring clinically healthy calves as healthy (Table 4-3 and 4-4). Sensitivity (between 54% and 60% for the three imaging modalities) and specificity (between 57% and 69% for the three imaging modalities) were similar for the less experienced evaluator. In comparison, the more experienced evaluator had a higher sensitivity (between 74% and 84% for the three imaging modalities) but a lower specificity (between 7% for US and 41% for CT) compared to histopathology.

Less experienced evaluator 1			**More experienced evaluator 2**		
	Histo Pos	Histo Neg		Histo Pos	Histo Neg
DR Pos	175	15	DR Pos	214	24
DR Neg	116	24	DR Neg	77	15
	Histo Pos	Histo Neg		Histo Pos	Histo Neg
US Pos	99	13	US Pos	142	14
US Neg	83	17	US Neg	28	1
	Histo Pos	Histo Neg		Histo Pos	Histo Neg
CT Pos	162	12	CT Pos	218	23
CT Neg	129	27	CT Neg	73	16

Table 4-3: Contingency tables assessing the diagnostic utility of DR, US and CT compared to histopathology as the reference standard.
Histo- histopathology, DR- Digital radiography, US- Ultrasound, CT- computed tomography, pos- positive, neg- negative

Modality	Evaluator	Sn (%)	95% CI	Sp (%)	95% CI	PPV	95% CI	NPV	95% CI	LR	LR p-val
DR	1	60	54-66	61	46-75	92	87-95	17	12-24	1.6	0.015
DR	2	74	68-78	38	25-54	90	85-93	16	10-25	1.2	0.13
US	1	54	47-61	57	39-73	88	81-93	17	11-26	1.3	0.325
US	2	84	77-88	7	0.3-30	91	86-95	3	0.2-17	0.9	0.473
CT	1	56	50-61	69	54-81	93	88-96	17	12-24	1.8	0.004
CT	2	75	70-80	41	27-57	90	86-94	18	11-27	1.3	0.053

Table 4-4: Sensitivity, specificity, positive and negative predictive value and likelihood ratio including the confidence intervals of thoracic DR, pulmonary US and thoracic CT using histopathology as the reference standard.
Evaluator 1- less experienced evaluator, Evaluator 2- more experienced evaluator, Sn- sensitivity, Sp- specificity, PPV- positive predictive value, NPV- negative predictive value, 95% CI- 95% confidence interval, LR- likelihood ratio, p-val- p-value.

Imaging modalities performed similarly in accuracy using histopathology or group as the reference standard (Table 4-5). The exception to this was for evaluator 1 using CT where a higher accuracy (70%) was attained with group as the reference standard, and for evaluator 2 using CT where a higher accuracy (77%) was attained with histopathology as the reference standard.

	Evaluator 1		Evaluator 2	
	Histo	Group	Histo	Group
DR	57%	61%	71%	67%
US	60%	57%	69%	68%
CT	55%	70%	77%	72%

Table 4-5: Accuracy of imaging modalities arranged by evaluator and compared to histopathology (histo) or clinical health status (group) as reference standard.

4.3.6.2 Test Performance of the Imaging Modalities Compared to Clinical Status (HEALTH or PNEUM Group)

Using clinical disease status as reference standard (Tables 4-5 to 4-7), the accuracy of clinical disease detection by the more experienced evaluator was similar for the three imaging modalities (DR: 67%, US: 68%, CT: 72%). For the less experienced evaluator, the accuracy was higher with CT (70%) compared with DR (61%) and US (57%) (Table 4-6).

When using clinical status has a reference standard, both evaluators were better in differentiating the clinically healthy from the diseased calves (Table 4-6) than when using histopathology as a reference standard. Sensitivity (between 57% and 71% for the three imaging modalities) and specificity (between 57% and 71% for the three imaging modalities) were similar for the less experienced evaluator. In comparison, the more experienced evaluator had a higher sensitivity (between 77% and 84% for the three imaging modalities) but a lower specificity (between 14% for US and 48% for CT).

Less experienced evaluator 1			**More experienced evaluator 2**		
	Histo Pos	Histo Neg		Histo Pos	Histo Neg
DR Pos	151	39	DR Pos	185	54
DR Neg	89	51	DR Neg	55	36
	Histo Pos	Histo Neg		Histo Pos	Histo Neg
US Pos	91	21	US Pos	119	37
US Neg	71	29	US Neg	23	6
	Histo Pos	Histo Neg		Histo Pos	Histo Neg
CT Pos	157	17	CT Pos	194	47
CT Neg	83	73	CT Neg	46	43

Table 4-6: Contingency tables assessing the diagnostic utility of DR and US compared with clinical health status (group) as the reference standard.
DR- DR, US- Ultrasound, CT- computed tomography, pos- positive, neg- negative

Modality	Evaluator	Sn (%)	95% CI	Sp (%)	95% CI	PPV	95% CI	NPV	95% CI	LR	LR p-val
DR	1	63	57-69	57	46-66	79	73-85	36	29-45	1.45	0.002
DR	2	77	71-82	40	30-50	77	72-82	40	30-50	1.29	0.004
US	1	56	48-64	58	44-71	81	73-87	29	21-39	1.34	0.105
US	2	84	77-89	14	7-27	76	69-82	21	10-38	0.97	0.815
CT	1	65	59-71	81	72-88	90	85-94	47	39-55	3.46	<0.0001
CT	2	81	75-85	48	38-58	81	75-85	48	38-59	1.55	<0.0001

Table 4-7: Sensitivity, specificity, positive and negative predictive value and likelihood ratio including the confidence intervals of lung DR, US and CT using clinical health status (group) as the reference standard.
1- less experienced evaluator, 2- more experienced evaluator, Sn- sensitivity, Sp- specificity, PPV- positive predictive value, NPV- negative predictive value, 95% CI- 95% confidence interval, LR- likelihood ratio, p-val- p-value.

4.3.7. Other Findings Including Pleural Fluid and Cavitary Structures

Eight calves (7 PNEU, 1 HEALTH) were diagnosed with air-filled cavitary structures on CT examination. Three of these were confirmed by histopathology as one bulla and two air-filled abscesses. Four air-filled cavitary structures were seen on DR, with only two being confirmed by CT and histopathology. No air-filled cavitary regions were detected by US. The bulla seen on necropsy was also detected on both CT and DR, and was the largest cavitary structure seen in the study. This bulla was not identified on US as it was located on the dorsomedial aspect of the lung lobe and therefore not accessible (Fig 4-8).

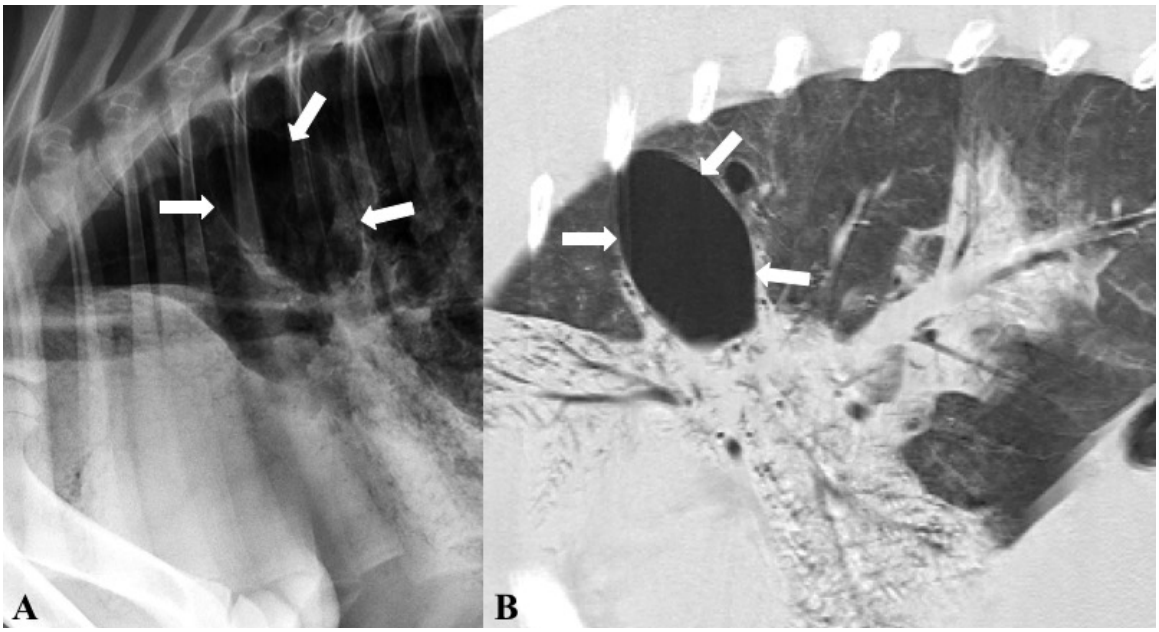

Figure 4-8: Large bulla detected on DR and CT. Standing lateral radiograph (A) and sagittal plane CT image in bone window (B) of the thorax with a very large bulla (white arrows).

Pleural fluid was not identified in any of the calves in either group using imaging or histopathology.

4.4 Discussion

The Wisconsin RS system differentiated between clinically healthy and diseased calves, with the exception of one diseased calf, which had a RS of 3. Coughing was not seen in any of the HEALTH group calves and present in all of the PNEUM group calves, suggesting this may be an easily detectible sign of respiratory disease in calves. Despite the ability to differentiate the HEALTH group from the PNEUM group, all calves considered clinically healthy had focal areas of pulmonary changes consistent with pneumonia, which were observed in all three imaging modalities by both evaluators and by histopathology. These changes were more mild in severity (imaging and histopathology score 2) and more prevalent in the cranial lung lobes in the HEALTH

group and more severe (imaging and histopathology score 3) in the ventral aspects of all lung lobes in the PNEUM group.

The *Trueperella sp.* growth on bacteriology cultures in two calves from the HEALTH group is likely due to the nasopharyngeal origin of the samples and likely represents a normal regional flora. The use of nasopharyngeal swabs for bacteriology culture is a shortcoming for assessment of the HEALTH group. Utilizing samples of lung tissue for bacteriology culture was planned in these cases, but were not performed due to a sample processing error. In future studies, additional efforts should be placed on ensuring sample consistency between clinical groups by directly culturing lung tissue for better correlation of bacteriologic results to the histopathology and imaging findings.

The large number of histopathologically abnormal lung samples from the clinically healthy calves was not expected to this extent. Pathologies in the right cranial lung lobes were expected due to its tracheal bronchus and its reported common site of changes consistent with pneumonia.(21) The PNEUM group calves were more likely to have consolidation or necrosis, a more common histopathologic finding in pneumonia, and these histopathologic findings were never or rarely seen in the HEALTH group calves. The largest group of imaging findings and histopathologic findings fall into the interstitial to bronchial group in both groups and the biologic significance of interstitial and bronchial lung tissue changes in clinically healthy calves is unclear.

For clinically healthy calves, the most severe and largest region of pulmonary parenchymal change was present in the most cranial aspect of the lung; these changes were observed by all imaging modalities by both imaging evaluators as well as by the pathologist. Due to the shape of the US transducer utilized in this study, the cranial lung

deep to the front limbs could not be imaged by US. This is similar to previous reports in which portions of the lungs cranial to the fourth rib were not being imaged by US.(23) This represents regional limitation of US and may be a source of false negative diagnoses in calves with early or localized disease considering the predilection of lung parenchymal changes in the cranial lung lobes. This limitation may be overcome by utilizing a linear transducer intended for rectal imaging.(24)

Generally, the less experienced imaging evaluator (Evaluator 1) was less sensitive for detection of pulmonary disease, but had an overall higher specificity and likelihood ratio. This was for the less experienced imaging evaluator most noticeable for CT and suggests that a less experienced evaluator may be less likely to call imaging abnormalities as diseased. The more experienced evaluator had a substantially higher sensitivity with all modalities, especially US, but this was on cost of specificity. Thus, a, more experienced evaluator may be more likely to diagnose a clinically healthy calf with pulmonary disease; which is consistent with the histopathology results. Although high sensitivity for respiratory disease detection is beneficial for starting early treatment and potentially preventing the spread of respiratory disease, having a high false positive rate is detrimental in that it may lead to administration of antibiotics to calves without bacterial infections and additional costs for producers without medical benefit to the calf.

The cause of the less experienced imaging evaluator scoring more clinically healthy calves as having a normal lung despite abnormalities lung histopathology is not entirely clear. One potential explanation is that less experienced image evaluators may mistake an interstitial pattern in combination with motion as normal. Both imaging evaluators were similarly successful to detect severe histopathology changes (i.e.,

alveolar patterns) with DR. Image differences between normal and alveolar pathology are in comparison to interstitial versus normal pathology strong, which allows less experienced imaging evaluators accurate diagnosis of alveolar lung patterns in calves.

Abnormal B-lines and white lung were seen in US images in all of the calves in the study, including clinically healthy calves. In a human study comparing thoracic ultrasound with CT and DR, US was accurate in diagnosis of pneumonia, with a 100% diagnosis rate compared with CT. In contrast, DR was only accurate in diagnosing 52% of the pneumonia cases identified by CT.(25) In the current study, a similar diagnostic rate was seen in all three imaging modalities for a given evaluator as seen in table 4-4. Moreover, all clinically diseased calves had multiple lung sites diagnosed as abnormal pathology with all three imaging modalities by both imaging evaluators. A limitation is that multiple lung sites in clinical healthy calves were also scored by histopathology and imaging modalities as indicative of pneumonia, which decreased the specificity of disease detection.

US was limited in the evaluation of cavitary structures; the largest bulla extended less than 0.1 cm from the pleural surface of the lungs but was not seen with US. This is not unsuspected for using ultrasound as lesions distal to normally aerated lung will not be visualized on ultrasound due to the lack of penetration of the ultrasound beam and the presence of reverberation artifacts. However, in regards to the changes noted with pneumonia in these study, the changes were extending to the pleural surface and therefore were visualized using ultrasound.

In contrast to Wisconsin RS scoring, thoracic US is a diagnostic tool used by veterinarians or skilled workers. Despite the costs associated with the equipment, the

flexibility of US and the absence of ionizing radiation makes it a potential modality for cattle management.

CT examination allowed for a global overview of the parenchymal changes associated with respiratory disease. CT was able to identify severe structural abnormalities, specifically bullae and abscesses. The cavitary structures seen in five calves on CT were not corroborated on necropsy, which has several potential explanations including that the pathologist may miss the cavitary structures because of loss of air filling post-mortem or a lack of change in the contour of the lung or the number of samples obtained from each calf was insufficient for detection. One clinically healthy calf had a bullous structure as identified on CT only. Whether this structure was a congenital bulla, or a structure developed from previous disease could not be distinguished.

In this study, thoracic DR, pulmonary US, and thoracic CT performed similarly well for pneumonia detection by each evaluator, and a more experienced evaluator had a better overall sensitivity for disease detection with all imaging modalities. This supports the use of US for the on-farm examination of at-risk calves or those with an acute onset of cough.

4.5 Footnotes

[a]CXDI-701C; Canon Inc., Tokyo, Japan
[b] Noblus; Hitachi Aloka Medical America Inc., Wallingford, CT
[c]Ketaset®, Pfizer/Boehringer, St. Joseph, MO
[d]Anased®, Lloyd Laboratories, Shenandoah, IA
[e]Torbugesic®, Pfizer, New York, NY
[f] Toshiba Aquilion 64, Toshiba America Medical Systems Inc., Tustin, CA
[g]Isovue 300, Bracco Diagnostics Inc., Princeton, NJ
[h] Empower CTA, Bracco Diagnostics Inc., Princeton, NJ
[i]Beuthanasia ®-D Special, Schering-Plough Animal Health Corp, Union, NJ

[j]eFilm, version 3.3.0, Merge Healthcare, Hartland, WI
[k]Vitrea workstation, software version 6.3.2, Vital Images Inc., Minnetonka, MN
[l]GraphPad Prism, version 7.0b, GraphPad Software Inc., La Jolla, CA
[m]SAS version 9,2, SAS Institute Inc., Cary, NC

4.6 References

1. Cernicchiaro N, White BJ, Renter DG, Babcock AH. Evaluation of economic and performance outcomes associated with the number of treatments after an initial diagnosis of bovine respiratory disease in commercial feeder cattle. Am J Vet Res. 2013;74(2):300–9.
2. USDA:APHIS:VS. Dairy Heifer Raiser, 2011. Fort Collins, CO; 2012.
3. USDA Veterinary Services - Centers for Epidemiology and Animal Health. Feedlot 2011: Types and Costs of Respiratory Disease Treatments in U.S. Feedlots [Internet]. 2013. Available from: https://www.aphis.usda.gov/animal_health/nahms/feedlot/downloads/feedlot2011/Feed11_is_RespDis.pdf
4. USDA. Dairy 2007 - Heifer calf health and Management practices on U.S. Operations. USDAAPHISVS,CEAH Fort Collins, CO [Internet]. 2010;(January):168. Available from: http://www.aphis.usda.gov/animal_health/nahms/dairy/downloads/dairy07/Dairy07_ir_CalfHealth.pdf
5. Thomas LH, Scott EJ, Collins AP, Jebbett NJ, Stark AJ. Evaluation of respiratory disease in calves: comparison of disease response to different viruses. Res Vet Sci. 1977;23:157–64.
6. McGuirk SM, Peek SF, McGuirk , Sheila M.; Peek SF, McGuirk SM, Peek SF. Timely diagnosis of dairy calf respiratory disease using a standardized scoring system. Anim Heal Res Rev. 2014;15(2):145–7.
7. Panciera RJ, Confer AW. Pathogenesis and pathology of bovine pneumonia. Veterinary Clinics of North America - Food Animal Practice. 2010.
8. Love WJ, Lehenbauer TW, Van Eenennaam AL, Drake CM, Kass PH, Farver TB, et al. Sensitivity and specificity of on-farm scoring systems and nasal culture to detect bovine respiratory disease complex in preweaned dairy calves. J Vet Diagn Invest [Internet]. 2016;28(2):119–28. Available from: http://vdi.sagepub.com/content/28/2/119
9. Amrine DE, White BJ, Larson R, Anderson DE, Mosier DA, Cernicchiaro N. Precision and accuracy of clinical illness scores, compared with pulmonary consolidation scores, in Holstein calves with experimentally induced Mycoplasma bovis pneumonia. Am J Vet Res. 2013;
10. Lynch T, Bialy L, Kellner JD, Osmond MH, Klassen TP, Durec T, et al. A systematic review on the diagnosis of pediatric bacterial pneumonia: When gold is bronze. PLoS One. 2010;5(8).
11. Rizzi EB, Schinina' V, Cristofaro M, Goletti D, Palmieri F, Bevilacqua N, et al. Detection of Pulmonary tuberculosis: comparing MR imaging with HRCT. BMC Infect Dis [Internet]. 2011;11:243. Available from:

http://www.pubmedcentral.nih.gov/articlerender.fcgi?artid=3184086&tool=pmcentrez&rendertype=abstract
12. Ohlerth S, Augsburger H, Abe M, Ringer S, Hatz L, Braun U. Computed tomography of the thorax in calves from birth to 105 days of age. Schweiz Arch Tierheilkd. 2014;156(10):489–97.
13. Lubbers B V., Apley MD, Coetzee JF, Mosier DA, Biller DS, Mason DE, et al. Use of computed tomography to evaluate pathologic changes in the lungs of calves with experimentally induced respiratory tract disease. Am J Vet Res. 2007;68(11):1259–64.
14. Flöck M. Diagnostic ultrasonography in cattle with thoracic disease. Vet J. 2004;
15. Reef VB, Whittier M, Allam LG. Thoracic Ultrasonography. Clin Tech Equine Pr. 3:284–93.
16. Poulsen KP, McGuirk SM. Respiratory Disease of the Bovine Neonate. Veterinary Clinics of North America - Food Animal Practice. 2009.
17. Rademacher N, Pariaut R, Pate J, Saelinger C, Kearney MT, Gaschen L. Transthoracic lung ultrasound in normal dogs and dogs with cardiogenic pulmonary edema: A pilot study. Vet Radiol Ultrasound. 2014;55(4):447–52.
18. Jean D, Picandet V, Macieira S, Beauregard G, D'Anjou M a, Beauchamp G. Detection of rib trauma in newborn foals in an equine critical care unit: a comparison of ultrasonography, radiography and physical examination. Equine Vet J. 2007;39(2):158–63.
19. Calf Respiratory Score [Internet]. University of Wisconsin. Available from: https://www.vetmed.wisc.edu/dms/fapm/fapmtools/8calf/calf_respiratory_scoring_chart.pdf
20. McGuirk SM. Disease Management of Dairy Calves and Heifers. Vet Clin North Am - Food Anim Pract. 2008;24(1):139–53.
21. Veit HP, Farrell RL. The anatomy and physiology of the bovine respiratory system relating to pulmonary disease. Cornell Vet. 1978;68:555–81.
22. Doster AR. Bovine Atypical Interstitial Pneumonia. Vet Clin NA Food Anim Pract [Internet]. Elsevier Ltd; 2010;26(2):395–407. Available from: http://dx.doi.org/10.1016/j.cvfa.2010.03.002
23. Buczinski S, L Ollivett T, Dendukuri N. Bayesian estimation of the accuracy of the calf respiratory scoring chart and ultrasonography for the diagnosis of bovine respiratory disease in pre-weaned dairy calves. Prev Vet Med. 2015;
24. Ollivett T. Understanding the Diagnosis and Risk Factors for Respiratory Disease in Dairy Calves. 2014.
25. Bourcier JE, Paquet J, Seinger M, Gallard E, Redonnet JP, Cheddadi F, et al. Performance comparison of lung ultrasound and chest x-ray for the diagnosis of pneumonia in the ED. Am J Emerg Med. 2014;32(2):115–8.

Chapter 5- Conclusions and Future Directions

As diagnostic imaging allows for a relatively non-invasive method for examination of the pulmonary parenchyma, understanding the limitations of image acquisition and the accuracy of the imaging modalities (i.e., radiography, computed tomography, and ultrasonography) for diagnosing calf respiratory disease remains an important consideration.

The work presented in Chapter 3 compared computed radiography with a novel sedated MDCT protocol and the Wisconsin Calf Respiratory Scoring system for pneumonia detection in calves with acute or chronic respiratory disease. Our results showed that both imaging modalities were equally effective in detecting pneumonia in calves; however, a less experienced image evaluator may underscore lung disease severity. Furthermore, it is feasible and safe to perform contrast enhanced CT of the thorax of sedated dairy calves with naturally acquired pneumonia. The CT images acquired in this study had mild respiratory motion artifacts on average, which did not impede pneumonia diagnosis in calves. A limitation of both imaging modalities is the use of ionizing radiation.

The work presented in Chapter 4 compared a pulmonary US for pneumonia detection in clinical healthy and respiratory diseased calves with thoracic CR, CT, and the Wisconsin Calf Respiratory Scoring system. Pulmonary US was shown to be a simple and quick method for pneumonia diagnosis in calves without animal handler exposure to ionizing radiation. However, US did not allow identification of intraparenchymal bullae or abscesses. Although clinically healthy calves showed pulmonary pathologies, the biological importance of the changes are unknown. The environmental bacterial and

Trueperella pyogenes growth seen on bacteriology cultures from the group of clinically healthy calves is normal given that the samples were obtained from the pharyngeal region. As such, the degree of changes seen on diagnostic imaging and histopathology could be due to interstitial pneumonia that may resolve on its own, or indicate a normal pulmonary response to environmental particles including dust and pollen in the absence of a biologically active infection. Thoracic CT allowed for the best global over-view of the thoracic structures and detected more air-filled cavitary structures than necropsy, CR, or US.

In both studies, pneumonia detection was similar across imaging modalities within imaging evaluators, but a more experienced image evaluator is able to differentiate mild interstitial pathology from motion artifacts. The Wisconsin Calf Respiratory Scoring method employed in these studies has again been shown to be insensitive for detecting patients with long-term chronic pneumonia. This insensitivity is consistent with the fact that respiratory scoring is designed as a tool for acute disease diagnosis.

Further studies examining the impact of evaluator training and experience may be helpful for better understanding the potential for employing thoracic ultrasonography as a complementary on-farm herd surveillance tool. For example, one method by which to consider thoracic ultrasonography as a herd surveillance tool may be by combining an abbreviated thoracic fast scan technique with an abbreviated clinical scoring method. Additionally, as linear rectal transducers are more commonly available to farm service veterinarians, further examining the differences in image quality and diagnostic accuracy between rectal and linear transducers is indicated to better enable comparison of results of previous research.

5.1 Comparison of imaging modalities for evaluating the lungs in bovine patients

The primary benefits and limitations of diagnostic imaging modalities was previously described (Table 1-1). Based on the findings from the studies described in Chapter 3 and Chapter 4, further comparisons of the diagnostic utility of each imaging modality for diagnosing naturally acquired pneumonia in calves are summarized (Table 5-1).

	Benefits	Limitations
Radiography	-similar diagnostic performance to CT and US -Accuracy 55-75%, with experience improving accuracy	- exposure to ionizing radiation of calf and personnel
Computed Tomography	-Accuracy 55-77%, with experience improving accuracy	-ionizing radiation exposure to calf - facility dependent personnel exposure to ionizing radiation
Ultrasonography	-Accuracy 60-72%, with experience improving accuracy -No exposure to ionizing radiation for patient or personnel	-Cannot assess the dorsal portions of the cranial lung lobes, the accessory lung lobe, or deep parenchymal structures such as bullae, abscesses, etc.

Table 5-1: Comparison of the benefits and limitations of the various imaging techniques evaluating the lungs in calves.